List of Supplemental Tables

List of Supplemental Figures

Supplementary Table 1. Summary of changes in mHTT levels for different durations of m*Htt* lowering using LacQ140 mice

				6 month striatum					9 month striatum			
				LacQ140_A vs. LacQ140		LacQ140_2M vs. LacQ140			LacQ140_A vs. LacQ140		LacQ140_2M vs. LacQ140	
	HTT epitope			% lower	P value	% lower	P value		% lower	P value	% lower	P value
Ab1	aa1-17	Wes	Q7 HTT		N.S.		N.S.			N.S.		N.S.
			Q140 HTT	43%	<0.01	38%	<0.01		52%	<0.01	42%	<0.01
MW1	polyQ	Wes	Q140 HTT	47%	<0.01	40%	<0.01		43%	<0.001	44%	<0.001
EPR5526	N-terminal HTT	Western blot	Q7 HTT		N.S.		N.S.			N.S.		N.S.
			Q140 HTT		N.S.		N.S.		30%	<0.01	24%	<0.05
PHP3	Proline rich domain	Western blot	Q140 HTT	35%	<0.01	42%	<0.001		49%	<0.001	46%	<0.001

				12 month striatum						
				Group comparison, p value						
	HTT epitope			LacQ140_A vs. LacQ140	LacQ140_A vs. WT	LacQ140_A vs. LacQ140_2M	LacQ140_A vs. LacQ140_8M	LacQ140 vs. WT	LacQ140_2M vs. WT	LacQ140_8M vs. WT
Ab1	aa1-17	Wes	Q7 HTT	N.S.	<0.001	<0.05	<0.05	<0.001	<0.01	<0.01
			Q140 HTT	<0.01	-	N.S.	N.S.	-	-	-
MW1	polyQ	Wes	Q140 HTT	N.S.	-	N.S.	N.S.	-	-	-
EPR5526	N-terminal HTT	Western blot	Q7 HTT	N.S.	N.S.	N.S.	N.S.	<0.01	<0.01	N.S.
			Q140 HTT	N.S.	-	N.S.	N.S.	-	-	-
PHP3	Proline rich domain	Western blot	Q140 HTT	N.S.	-	N.S.	N.S.	-	-	-

Supplementary Table 2. Proteins altered by m*Htt* lowering for different periods using LacQ140 mice

	6 month striatum					
	Group comparison, p value					
	LacQ140_A vs. LacQ140	LacQ140_A vs. WT	LacQ140_A vs. LacQ140_2M	LacQ140 vs. WT	LacQ140_2M vs. LacQ140	LacQ140_2M vs. WT
PDE10	<0.001	N.S.	<0.05	<0.001	<0.01	N.S.
SCN4B	N.S.	N.S.	N.S.	<0.01	<0.05	N.S.
GFAP	N.S.	N.S.	N.S.	N.S.	N.S.	N.S.
DARPP32	N.S.	N.S.	N.S.	N.S.	N.S.	N.S.
ATP5A	N.S.	N.S.	N.S.	N.S.	N.S.	N.S.

	9 month striatum					
	Group comparison, p value					
	LacQ140_A vs. LacQ140	LacQ140_A vs. WT	LacQ140_A vs. LacQ140_2M	LacQ140 vs. WT	LacQ140_2M vs. LacQ140	LacQ140_2M vs. WT
PDE10	N.S.	<0.01	<0.01	<0.001	<0.001	N.S.
SCN4B	<0.05	<0.01	N.S.	<0.001	<0.01	<0.05
GFAP	<0.05	N.S.	N.S.	N.S.	N.S.	N.S.
DARPP32	N.S.	<0.01	N.S.	<0.001	N.S.	<0.001
ATP5A	<0.001	<0.01	N.S.	N.S.	<0.001	<0.05

	12 month striatum					
	Group comparison, p value					
	LacQ140_A vs. LacQ140	LacQ140_A vs. LacQ140_2M	LacQ140_A vs. LacQ140_8M	LacQ140 vs. WT	LacQ140_2M vs. WT	LacQ140_8M vs. WT
PDE10	<0.01	<0.05	N.S.	<0.001	<0.05	<0.05
SCN4B	N.S.	N.S.	N.S.	N.S.	N.S.	N.S.
GFAP	N.S.	N.S.	N.S.	N.S.	N.S.	N.S.
DARPP32	N.S.	<0.05	<0.05	N.S.	N.S.	N.S.
ATP5A	N.S.	N.S.	N.S.	N.S.	N.S.	N.S.

Supplementary Table 3. Individual lipid species significantly different between any treatment group in 6-month-old mice (p<0.05)

Category	Subclass	Lipid Species	m/z	Formula	ANOVA	Adjusted p-value (q) n = 800
Glycerophospholipids	**PC**	PC(19:1_16:0)+H	774.6007335	C43 H85 O8 N1 P1	F (3, 20) = 4.352, *P=0.0163	1
	PE	PE(18:1p_20:4)+H	750.5432185	C43 H77 O7 N1 P1	F (3, 20) = 3.300, *P=0.0414	1
	PE	PE(18:0p_18:1)+H	730.5745185	C41 H81 O7 N1 P1	F (3, 20) = 3.108, *P=0.0496	1
	PS	PS(22:6_22:6)-H	878.4977605	C50 H73 O10 N1 P1	F (3, 20) = 3.498, *P=0.0346	1
	PS	PS(18:0_20:4)-H	810.5290605	C44 H77 O10 N1 P1	F (3, 20) = 3.349, *P=0.0396	1
	PS	PS(18:0_18:1)+H	790.5592635	C42 H81 O10 N1 P1	F (3, 20) = 3.297, *P=0.0416	1
	PI	PI(18:0_20:4)+NH4	904.5909585	C47 H87 O13 N1 P1	F (3, 20) = 3.812, *P=0.0260	1
	PI	PI(16:0_22:6)-H	881.5185565	C47 H78 O13 N0 P1	F (3, 20) = 3.466, *P=0.0356	1
	CL	CL(22:6_18:1_18:1_22:6)-2H	773.494489	C89 H144 O17 P2	F (3, 20) = 4.096, *P=0.0203	1

Supplementary Table 4. Individual lipid species significantly different between 9-month-old LacQ140 and WT mice (q<0.05).

Category	Subclass	Lipid Species	m/z	Formula	ANOVA	Adjusted p-value (q) n = 632
Glycerophospholipids	**PC**	PC(36:5e)+H	766.5745185	C44 H81 O7 N1 P1	F (3, 20) = 10.68, ***P=0.0002	0.02039117
	PE	PE(16:1e_20:4)-H	722.5130155	C41 H73 O7 N1 P1	F (3, 20) = 18.14, ***P<0.0001	0.00329333
	PE	PE(16:0p_20:4)+H	724.5275685	C41 H75 O7 N1 P1	F (3, 20) = 16.97, ***P<0.0001	0.00329333
	PI	PI(16:0_20:4)-H	857.5185565	C45 H78 O13 N0 P1	F (3, 20) = 8.449, ***P=0.0008	0.03984625
	PI	PI(18:1_20:4)+NH4	902.5753085	C47 H85 O13 N1 P1	F (3, 20) = 8.086, **P=0.0010	0.04159114
	PS	PS(18:0_20:4)-H	810.5290605	C44 H77 O10 N1 P1	F (3, 20) = 9.739.***P=0.0004	0.02386757
	PS	PS(18:0_18:1)-H	788.5447105	C42 H79 O10 N1 P1	F (3, 20) = 8.226, ***P=0.0009	0.04159114
	PS	PS(18:1_22:6)-H	832.5134105	C46 H75 O10 N1 P1	F (3, 20) = 7.916, **P=0.0011	0.04285691
Glycerolipids	**MGDG**	MGDG(16:0_18:1)+HCOO	801.5733535	C44 H81 O12	F (3, 20) = 11.28, ***P=0.0002	0.01957656
	TG	TG(8:2COOH_18:1_18:1)+H	773.5925965	C47 H81 O8	F (3, 20) = 11.98, ***P=0.0001	0.01785822
Sphingolipids	**Hex1Cer**	Hex1Cer(d18:1_18:0)+H	728.6034955	C42 H82 O8 N1	F (3, 20) = 10.37, ***P=0.0002	0.02039117
	Hex1Cer	Hex1Cer(t18:0_18:0)+H-H2O	728.6034955	C42 H82 O8 N1	F (3, 20) = 10.35, ***P=0.0003	0.02039117
	Hex1Cer	Hex1Cer(d18:1_25:1)+HCOO	868.6883225	C50 H94 O10 N1	F (3, 20) = 8.440, ***P=0.0008	0.03984625
	SM	SM(d40:2)+H	785.6531025	C45 H90 O6 N2 P1	F (3, 20) = 8.052, **P=0.0010	0.04159114

Supplementary Table 5. Individual lipid species significantly different between 12-month-old LacQ140 and WT mice (q<0.05).

Category	Subclass	Lipid Species	m/z	Formula	ANOVA	Adjusted p-value (q) n = 735
Glycerophospholipids	**PC**	PC(30:0)+H	706.5381335	C38 H77 O8 N1 P1	F (4, 25) = 7.601, ***P=0.0004	0.013150896
	PC	PC(20:3e_18:0)+H	798.6371185	C46 H89 O7 N1 P1	F (4, 25) = 5.567, **P=0.0024	0.032737797
	PE	PE(20:1_18:1)+H	772.5850835	C43 H83 O8 N1 P1	F (4, 25) = 10.36, ****P<0.0001	0.003802444
	PE	PE(16:0p_20:4)+H	724.5275685	C41 H75 O7 N1 P1	F (4, 25) = 7.879, ***P=0.0003	0.011411398
	PA	PA(36:3e)-H	683.5021165	C39 H72 O7 N0 P1	F (4, 25) = 13.27, ****P<0.0001	0.000660339
	PA	PA(36:2e)-H	685.5177665	C39 H74 O7 N0 P1	F (4, 25) = 5.630, **P=0.0023	0.032737797
Glycerolipids	**TG**	TG(16:0_18:1_18:2)+NH4	874.7858155	C55 H104 O6 N1	F (4, 25) = 8.357, ***P=0.0002	0.009358219
	TG	TG(16:0_16:0_18:1)+NH4	850.7858155	C53 H104 O6 N1	F (4, 25) = 7.833, ***P=0.0003	0.011411398
	TG	TG(18:1_18:1_18:2)+NH4	900.8014655	C57 H106 O6 N1	F (4, 25) = 7.113, ***P=0.0006	0.01823037
	TG	TG(18:0_16:0_18:1)+NH4	878.8171155	C55 H108 O6 N1	F (4, 25) = 6.726, ***P=0.0008	0.021749548
	TG	TG(18:1_18:2_18:2)+NH4	898.7858155	C57 H104 O6 N1	F (4, 25) = 6.249, **P=0.0013	0.027242438
	TG	TG(56:3+8O)+NH4	1058.807735	C59 H112 O14 N1	F (4, 25) = 6.109, **P=0.0014	0.027242438
	TG	TG(19:1_18:1_18:1)+NH4	916.8327655	C58 H110 O6 N1	F (4, 25) = 6.060, **P=0.0015	0.027242438
	TG	TG(16:0_16:1_18:1)+NH4	848.7701655	C53 H102 O6 N1	F (4, 25) = 5.794, **P=0.0019	0.030614623
	TG	TG(18:2_18:2_18:2)+NH4	896.7701655	C57 H102 O6 N1	F (4, 25) = 5.352, **P=0.0030	0.034548567
	TG	TG(16:1_18:1_18:2)+NH4	872.7701655	C55 H102 O6 N1	F (4, 25) = 4.983, **P=0.0043	0.043766147
Sphingolipids	**Hex1Cer**	Hex1Cer(d18:1_18:0+O)+H	744.5984105	C42 H82 O9 N1	F (4, 25) = 14.49, ****P<0.0001	0.000478321
	Hex1Cer	Hex1Cer(d40:2)+HCOO	826.6413725	C47 H88 O10 N1	F (4, 25) = 9.257, ****P<0.0001	0.005751743
	Hex1Cer	Hex1Cer(d41:2)+HCOO	840.6570225	C48 H90 O10 N1	F (4, 25) = 7.880, ***P=0.0003	0.011411398
	Hex1Cer	Hex1Cer(d18:1_22:1)+H	782.6504455	C46 H88 O8 N1	F (4, 25) = 6.637, ***P=0.0009	0.021916512
	Hex1Cer	Hex1Cer(t18:0_22:1)+H-H2O	782.6504455	C46 H88 O8 N1	F (4, 25) = 6.181, **P=0.0013	0.027242438
	Hex1Cer	Hex1Cer(d18:2_22:0+O)+H	798.6453605	C46 H88 O9 N1	F (4, 25) = 5.594, **P=0.0023	0.032737797
	SM	SM(d41:1)+HCOO	845.6753295	C47 H94 O8 N2 P1	F (4, 25) = 6.980, ***P=0.0006	0.019670123
	SM	SM(d18:1_23:0)+H	801.6844025	C46 H94 O6 N2 P1	F (4, 25) = 5.007, **P=0.0042	0.043766147
	CerP	CerP(t40:3)+CH3COO	772.5497955	C42 H79 O9 N1 P1	F (4, 25) = 14.26, ****P<0.0001	0.000478321
	ST	ST(d18:1_22:1)+H	862.6072625	C46 H88 O11 N1 S1	F (4, 25) = 6.263, **P=0.0012	0.027242438

Supplementary Table 6. Differentially expressed striatal transcripts related to sphingolipid metabolism, PI/PIP metabolism, glycerolipid metabolism, and myelin or oligodendrocytes in 6-month-old LacQ140 mice

Category	Gene	Description	Fold Change	FDR adj. p value
PI/PIP metabolism	Inpp4b	inositol polyphosphate-4-phosphatase, type II	-1.201960	1.01E-02
	Inpp5j	inositol polyphosphate 5-phosphatase J	-1.507014	9.86E-16
	Ippk	inositol 1,3,4,5,6-pentakisphosphate 2-kinase	-1.246942	4.23E-05
	Pigc	phosphatidylinositol glycan anchor biosynthesis, class C	-1.455025	1.05E-08
	Pik3c2b	phosphatidylinositol-4-phosphate 3-kinase catalytic subunit type 2 beta	-1.222034	2.01E-02
	Pik3r6	phosphoinositide-3-kinase regulatory subunit 5	-1.326717	1.44E-02
	Pla2g4c	phospholipase A2, group IVC (cytosolic, calcium-independent)	-3.049612	3.39E-02
	Pla2g7	phospholipase A2, group VII (platelet-activating factor acetylhydrolase, plasma)	-1.391677	4.64E-09
	Plcd4	phospholipase C, delta 4	-1.276632	3.97E-08
	Plcxd1	phosphatidylinositol-specific phospholipase C, X domain containing 1	-1.308018	1.47E-05
	Pld5	phospholipase D family, member 5	-1.221793	1.90E-03
	Plpp3	phospholipid phosphatase 3	-1.203758	5.52E-07
	Itpkc	inositol 1,4,5-trisphosphate 3-kinase C	1.208151	8.26E-04
	Nyap1	neuronal tyrosine-phosphorylated phosphoinositide 3-kinase adaptor 1	1.333238	4.15E-07
	Pla2g4e	phospholipase A2, group IVE	1.559296	1.10E-05
	Plcd3	phospholipase C, delta 3	1.304483	2.65E-09
	Pld6	phospholipase D family, member 6	1.274061	2.91E-02
	Plpp1	phospholipid phosphatase 1	1.240151	2.56E-08
	Plppr2	phospholipid phosphatase related 2	1.460144	8.46E-10
Sphingolipid metabolism	Arsg	arylsulfatase G	-1.249456	7.82E-06
	Asah1	N-acylsphingosine amidohydrolase 1	-1.213189	1.48E-04
	B4galt4	UDP-Gal:betaGlcNAc beta 1,4-galactosyltransferase, polypeptide 4	-1.272453	2.73E-10
	Elovl1	elongation of very long chain fatty acids (FEN1/Elo2, SUR4/Elo3, yeast)-like 1	-1.211314	1.02E-04
	Fa2h	fatty acid 2-hydroxylase	-1.349640	5.82E-05
	Gal3st4	galactose-3-O-sulfotransferase 4	-1.376902	3.48E-03
	Gba2	glucosidase beta 2	-1.305432	2.25E-14
	Ggta1	glycoprotein galactosyltransferase alpha 1, 3	-1.208597	1.47E-02
	Ormdl2	ORM1-like 2 (S. cerevisiae)	-1.230967	2.63E-02
	S1pr1	sphingosine-1-phosphate receptor 1	-1.284319	3.14E-11
	Sptssb	serine palmitoyltransferase, small subunit B	-1.569383	2.30E-02
	St3gal4	ST3 beta-galactoside alpha-2,3-sialyltransferase 4	-1.292839	2.89E-06
	St3gal6	ST3 beta-galactoside alpha-2,3-sialyltransferase 6	-1.206594	7.02E-03
	Ugt8a	UDP galactosyltransferase 8A	-1.659289	9.82E-09
	Gal3st3	galactose-3-O-sulfotransferase 3	1.225009	2.23E-03
	Smpdl3b	sphingomyelin phosphodiesterase, acid-like 3B	1.440528	4.01E-06
Glycerolipid metabolism	Dgat2l6	diacylglycerol O-acyltransferase 2-like 6	-2.873604	5.89E-10
	Gpat2	glycerol-3-phosphate acyltransferase 2, mitochondrial	-1.419945	4.83E-02
Myelin/oligodendrocyte related	Cldn11	claudin 11	-1.284516	9.74E-08
	Ermn	ermin, ERM-like protein	-1.356389	8.79E-07
	Mal	myelin and lymphocyte protein, T cell differentiation protein	-1.497728	4.28E-19
	Mbp	myelin basic protein	-1.210545	9.93E-06
	Plp1	proteolipid protein (myelin) 1	-1.456444	2.54E-18
	Pmp22	peripheral myelin protein 22	-1.266785	2.98E-06
	Tcf7l2	transcription factor 7 like 2, T cell specific, HMG box	-1.691672	1.16E-02

Supplementary Table 7. Differentially expressed striatal transcripts related to sphingolipid metabolism, PI/PIP metabolism, glycerolipid metabolism, and myelin or oligodendrocytes in 12-month-old LacQ140 mice.

Category	Gene	Description	Fold Change	FDR adj. p value
PI/PIP metabolism	Inpp5a	inositol polyphosphate-5-phosphatase A	-1.220035106	7.45E-13
	Inpp5j	inositol polyphosphate 5-phosphatase J	-1.746903179	2.29E-47
	Inppl1	inositol polyphosphate phosphatase-like 1	-1.430644212	8.13E-22
	Ippk	inositol 1,3,4,5,6-pentakisphosphate 2-kinase	-1.463777292	2.07E-19
	Isyna1	myo-inositol 1-phosphate synthase A1	-1.251503553	0.00604556
	Itpka	inositol 1,4,5-trisphosphate 3-kinase A	-1.423039308	4.58E-08
	Pdpk1	3-phosphoinositide dependent protein kinase 1	-1.23245825	0.000244656
	Pigc	phosphatidylinositol glycan anchor biosynthesis, class C	-1.284089248	4.26E-08
	Pik3c2b	phosphatidylinositol-4-phosphate 3-kinase catalytic subunit type 2 beta	-1.332729484	0.0000083
	Pitpnc1	phosphatidylinositol transfer protein, cytoplasmic 1	-1.277072463	0.00000166
	Pitpnm2	phosphatidylinositol transfer protein, membrane-associated 2	-1.6037997	2.12E-33
	Plcb1	phospholipase C, beta 1	-1.378055868	4.53E-08
	Plcb3	phospholipase C, beta 3	-1.208945654	0.000018
	Plce1	phospholipase C, epsilon 1	-1.269903756	0.0000595
	Plcl1	phospholipase C-like 1	-1.295458515	0.000208693
	Plcxd1	phosphatidylinositol-specific phospholipase C, X domain containing 1	-1.49232196	8.15E-11
	Pld5	phospholipase D family, member 5	-1.206041129	0.001149898
	Plpp3	phospholipid phosphatase 3	-1.203543891	0.004039833
	Plpp6	phospholipid phosphatase 6	-1.334745125	0.0000291
	Pigz	phosphatidylinositol glycan anchor biosynthesis, class Z	1.271675102	0.00601456
	Plaa	phospholipase A2, activating protein	1.225292039	0.0000279
	Pla2g4a	phospholipase A2, group IVA (cytosolic, calcium-dependent)	1.374559675	0.00023383
	Pla2g4e	phospholipase A2, group IVE	1.433879681	0.034925071
	Plpp1	phospholipid phosphatase 1	1.32803325	1.31E-11
	Plpp2	phospholipid phosphatase 2	1.479502814	0.000000017
	Plppr2	phospholipid phosphatase related 2	1.387816211	2.09E-08
Sphingolipid metabolism	B4galt2	UDP-Gal:betaGlcNAc beta 1,4- galactosyltransferase, polypeptide 2	-1.273957781	0.0000103
	Fa2h	fatty acid 2-hydroxylase	-1.291974775	0.001225211
	Gba2	glucosidase beta 2	-1.388099803	1.79E-19
	Ppara	peroxisome proliferator activated receptor alpha	-1.399564382	0.028802402
	Pparg	peroxisome proliferator activated receptor gamma	-1.461681387	0.040114102
	S1pr1	sphingosine-1-phosphate receptor 1	-1.299983738	0.00046959
	S1pr4	sphingosine-1-phosphate receptor 4	-1.768321775	0.005355694
	Sgms1	sphingomyelin synthase 1	-1.233983698	0.00000415
	Sgpp2	sphingosine-1-phosphate phosphotase 2	-1.254739263	0.008783654
	Smpd3	sphingomyelin phosphodiesterase 3, neutral	-1.367745501	4.17E-17
	St3gal2	ST3 beta-galactoside alpha-2,3-sialyltransferase 2	-1.233274708	0.00000317
	St3gal4	ST3 beta-galactoside alpha-2,3-sialyltransferase 4	-1.219568694	0.0000195
	Ugt8a	UDP galactosyltransferase 8A	-1.405539311	0.017983386
	Acer3	alkaline ceramidase 3	1.208246196	0.00193467
	B4galt6	UDP-Gal:betaGlcNAc beta 1,4-galactosyltransferase, polypeptide 6	1.215068033	0.000000425
	Cers4	ceramide synthase 4	1.245598312	0.000133202
	Gdap1l1	ganglioside-induced differentiation-associated protein 1-like 1	1.20387408	0.000106063
	Smpdl3b	sphingomyelin phosphodiesterase, acid-like 3B	1.239420969	0.0000114
Glycerolipid metabolism	Dagla	diacylglycerol lipase, alpha	-1.264855847	0.0000033
	Dgat2	diacylglycerol O-acyltransferase 2	-1.255826793	6.08E-08
	Dgat2l6	diacylglycerol O-acyltransferase 2-like 6	-3.730144224	9.96E-08
	Dgkb	diacylglycerol kinase, beta	-1.391179035	2.82E-08
	Dgki	diacylglycerol kinase, iota	-1.285596371	0.006874845
	Gpat2	glycerol-3-phosphate acyltransferase 2, mitochondrial	-2.323339721	5.75E-09
	Lpin3	lipin 3	-1.264610282	0.047484156
	Dgat1	diacylglycerol O-acyltransferase 1	1.20805369	0.018755728
	Dgka	diacylglycerol kinase, alpha	1.221574582	0.00868915
	Dgkg	diacylglycerol kinase, gamma	1.223769613	0.023533602
Myelin/oligodendrocyte related	Cldn11	claudin 11	-1.353046766	2.21E-10
	Mobp	myelin-associated oligodendrocytic basic protein	-1.330822203	0.000605929
	Mpzl3	myelin protein zero-like 3	-1.274933751	0.000133969
	Myt1l	myelin transcription factor 1-like	-1.342177794	0.00000605
	Plp1	proteolipid protein (myelin) 1	-1.377474017	0.000000137
	Olig1	oligodendrocyte transcription factor 1	1.215647167	0.004493267
	Omg	oligodendrocyte myelin glycoprotein	1.218646322	0.0000128
	Opalin	oligodendrocytic myelin paranodal and inner loop protein	1.515412385	0.000000898

Supplementary Figure 1

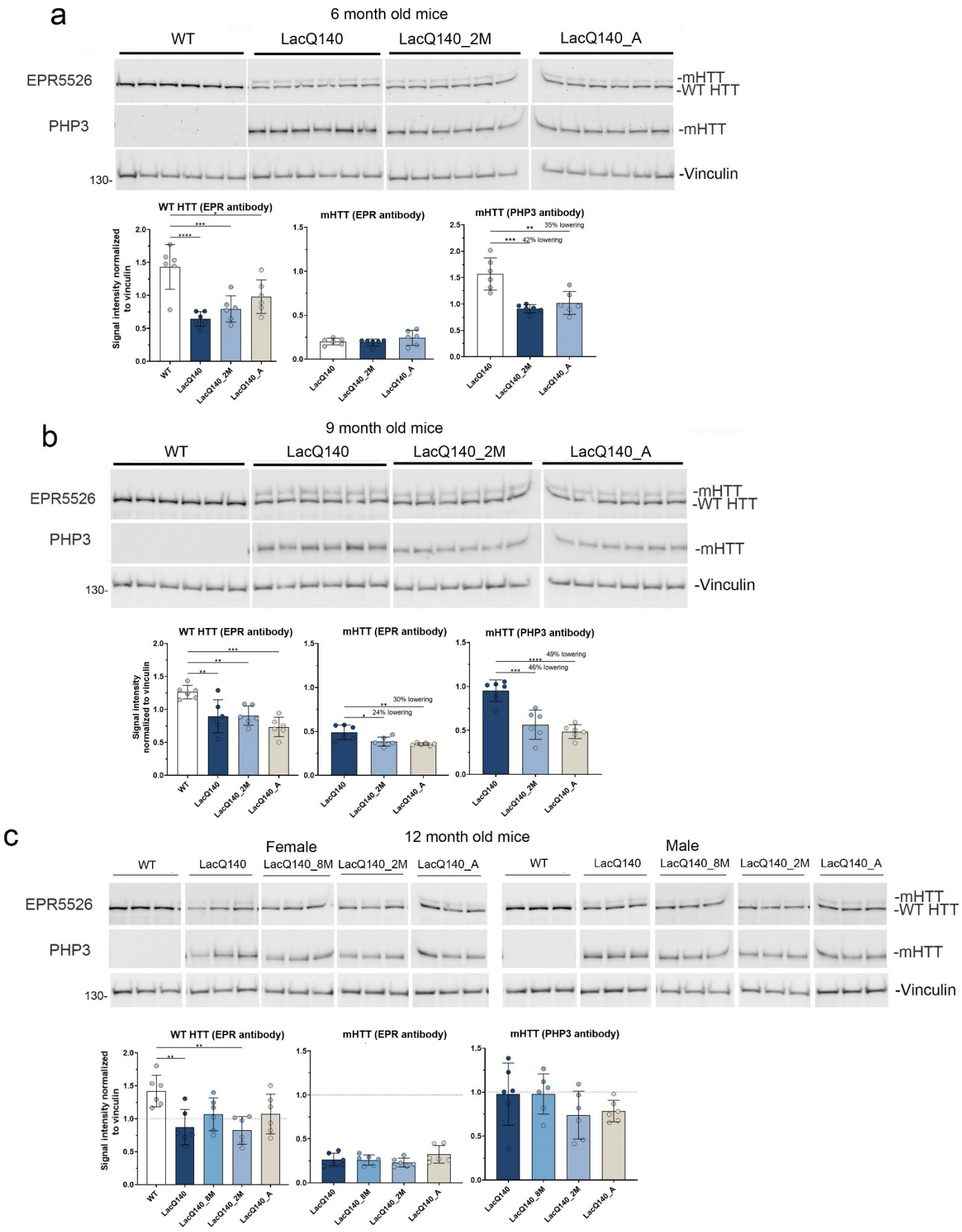

Supplementary Figure 1. Analysis of mHTT protein levels in crude homogenates of 6, 9 and 12 months old mice.

HTT levels were analyzed by western blot on equal amounts of protein (10 μg) using anti-HTT antibody EPR5526 and anti-polyQ antibody PHP3. Total pixel intensity quantification for each band measured using ImageJ software in 6 month old mice shows a significant decrease in WT HTT as detected with EPR5526 in all LacQ140 mice compared to WT mice but no change in mHTT levels (**a**). mHTT levels are significantly lower in LacQ140_2M and LacQ140_A mice as detected with PHP3 compared to LacQ140 (**a**, -42% and -35% respectively, **p<0.01, ***p<0.001, One-way ANOVA with Tukey's multiple comparison test, N=6).

Total pixel intensity quantification in 9 month old mice shows a significant decrease in WT HTT as detected with EPR5526 in all LacQ140 mice compared to WT mice. (**b**). mHTT levels are significantly lower in LacQ140_2M and LacQ140_A mice as detected with EPR5526 and PHP3 compared to LacQ140 (**b**, EPR5526: -24% and -30%, respectively; PHP3: -46% and -49% respectively, *p<0.05, **p<0.01, ***p<0.001, One-way ANOVA with Tukey's multiple comparison test, N=6).

Total pixel intensity quantification in 12 month old mice shows a significant decrease in WT HTT as detected with EPR5526 in LacQ140 and LacQ140_2M compared to WT mice. No changes in mHTT levels as detected with either EPR5526 or PHP3 were observed (**c**).

Supplementary Figure 2

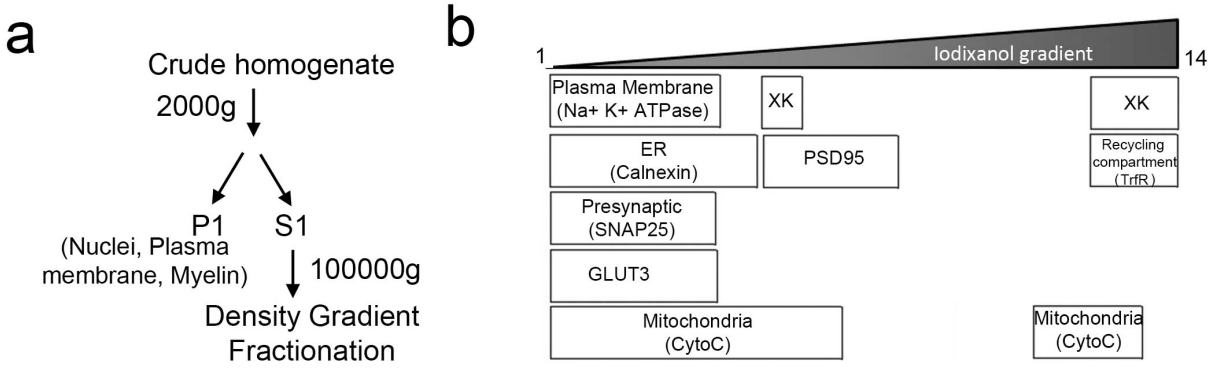

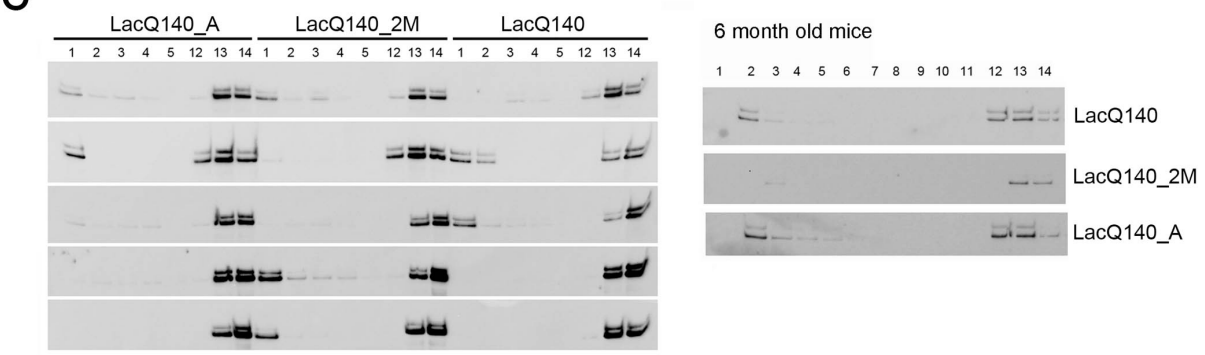

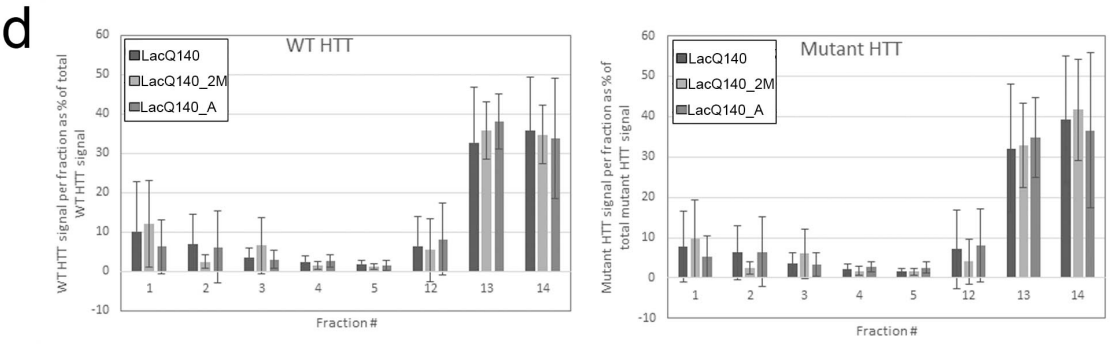

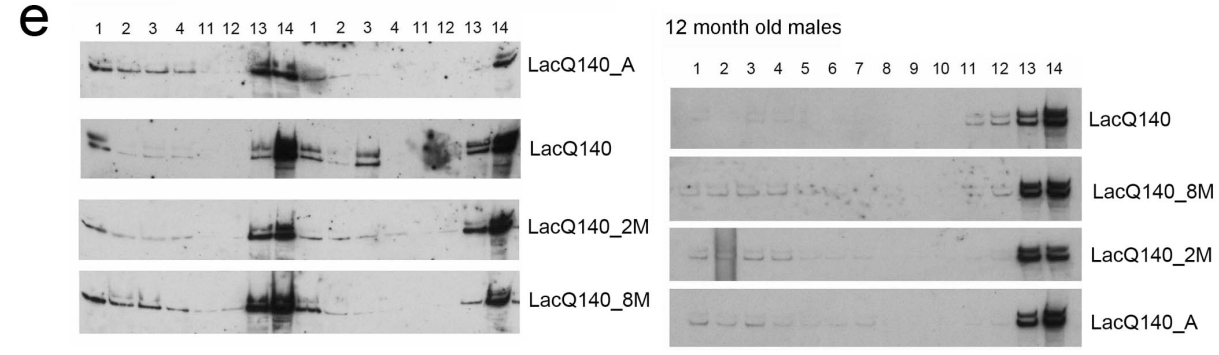

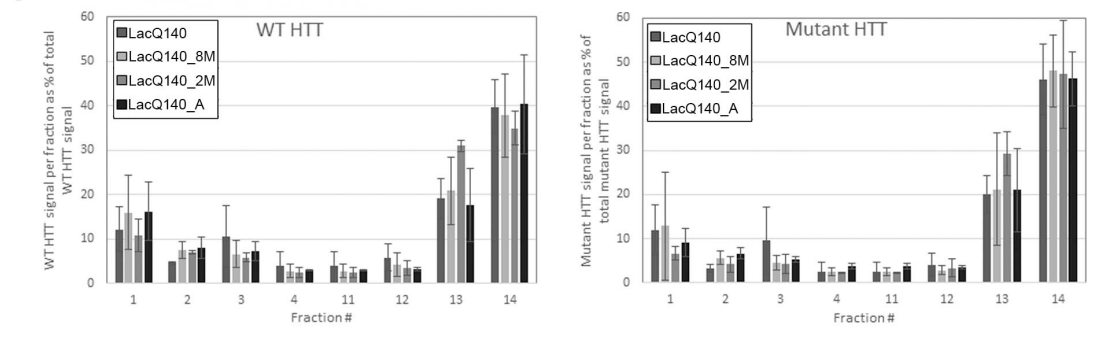

Supplementary Figure 2. Effects of m*Htt* lowering on the subcellular distribution of WT and mHTT by density gradient ultracentrifugation.

Diagram depicts the centrifugation strategy for protein samples (**a**). Schematic shows the approximate location in the fractions of protein markers and the organelles found in these compartments (**b**). Western blot images for equal volumes of fractions 1-14 (right blots, each strip is from one mouse) or fractions 1-5 and 12-14 (left blots) from 6-month-old mice probed with anti-HTT antibody Ab1 are shown in **c**. Each strip in left blots is a set of 1 mouse per treatment group with the groups labeled at the top of the blots. Total pixel intensity quantification for each band using ImageJ software is graphed as average percent of total HTT signal for each fraction ± SD (**d**). Representative western blot images for equal volumes of fractions 1-14 (right blots, each strip is from one mouse) or 1-4 and 11-14 (left blots) from 12-month-old mice probed with anti-HTT antibody Ab1 are shown in **e**. Each strip in the left blots is from 2 mice per group with the groups labeled on the right. Total pixel intensity quantified for each band using ImageJ software are graphed as average percent of total HTT signal for each fraction ± SD (**f**). There is no difference in WT or mHTT levels as a percent of total HTT in any fraction with any treatment of LacQ140 mice at 6 or 12 months (unpaired t test).

Supplementary Figure 3

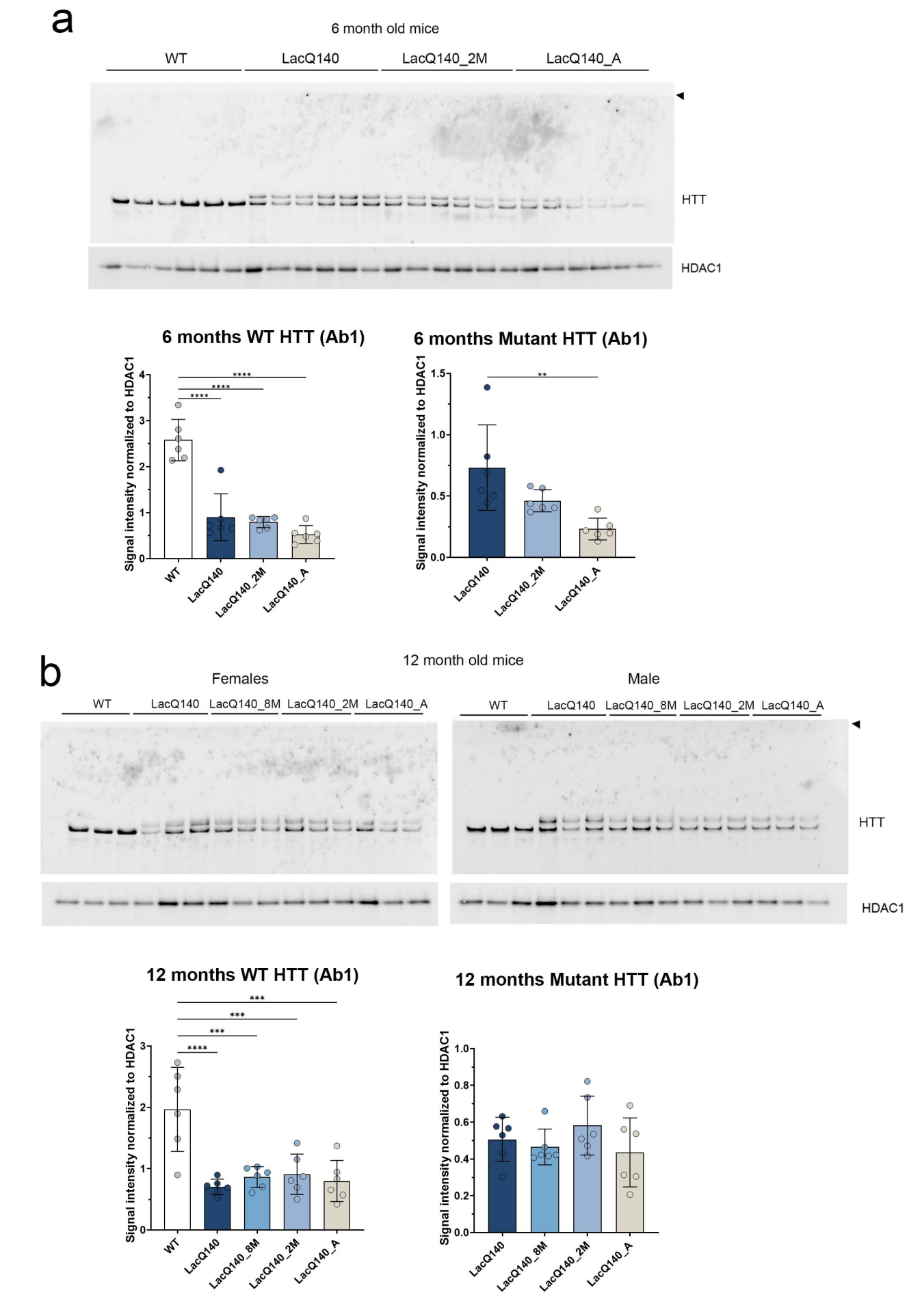

Supplementary Figure 3. HTT protein levels in P1 fractions. Equal protein (10 μg) from P1 fractions from 6-month-old (**a**) and 12-month-old (**b**) LacQ140 and WT mice were analyzed by western blot for HTT levels with anti-HTT Ab1. No aggregated protein was observed at the top of the gel (arrowhead). Total pixel intensity quantification for each band was measured using ImageJ software and normalized to HDAC1 signal. There was a significant decrease in WT HTT signal in all of the treatment conditions for LacQ140 mice compared to WT mice in both 6-month (**a**) and 12-month-old (**b**) mice (***p<0.001, One-way ANOVA with Tukey's multiple comparison test, n=6). There were significantly lower levels of mHTT in the 6-month-old LacQ140_A mice compared to LacQ140 (**a,** **p<0.01, One-way ANOVA with Tukey's multiple comparison test, n=6) but no changes in mHTT levels were detected in the 12 month old LacQ140 mice (**b**).

Supplementary Figure 4

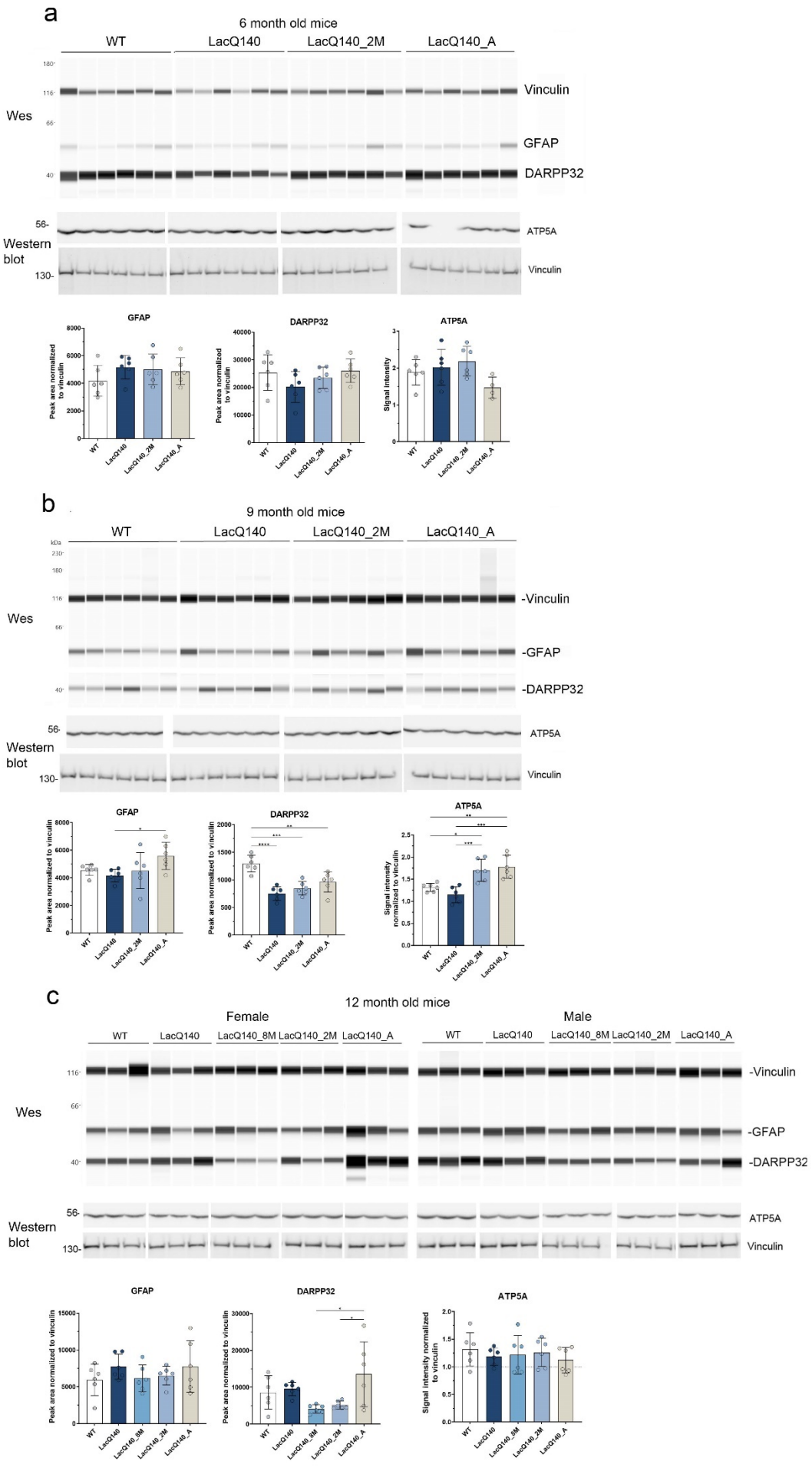

Supplementary Figure 4. Duration of m*Htt* lowering in 6, 9 and 12 months old LacQ140 mice has minimal effects on levels of GFAP, DARPP32 and ATP5A.

GFAP and DARPP32 levels were analyzed by capillary immunoassay on equal amounts of protein (0.6 mg) and ATP5A levels were analyzed by western blot on equal amounts of protein (10 mg). In 6-month-old mice, peak area analysis shows no significant change in GFAP or DARPP32 levels (**a**) and total pixel intensity quantification shows no changes in ATP5A levels in any of the LacQ140 or WT mice (**a**).

Peak area analysis in 9 month old mice shows a significant increase in GFAP levels in LacQ140_A compared to WT mice. There was a significant decrease in DARPP32 levels in all LacQ140 mice compared to WT (**b**, **p<0.05, **p<0.01, ***p<0.001, One-way ANOVA with Tukey's multiple comparison test, n=6). Total pixel intensity quantification shows ATP5A levels are significantly higher in LacQ140_2M and LacQ140_A mice compared to WT or LacQ140 mice (**b,** *p<0.05, **p<0.01, ***p<0.001, One-way ANOVA with Tukey's multiple comparison test, n=6).

Peak area analysis in 12-month-old mice shows no significant change in GFAP levels in LacQ140 or WT mice. There is a significant decrease in DARPP32 levels in LacQ140_8M and LacQ140_2M compared to LacQ140_A mice (**c,** *p<0.05, One-way ANOVA with Tukey's multiple comparison test, n=6). Total pixel intensity quantification for each band using ImageJ software shows no changes in ATP5A levels in any of the LacQ140 or WT mice.

Supplementary Figure 5

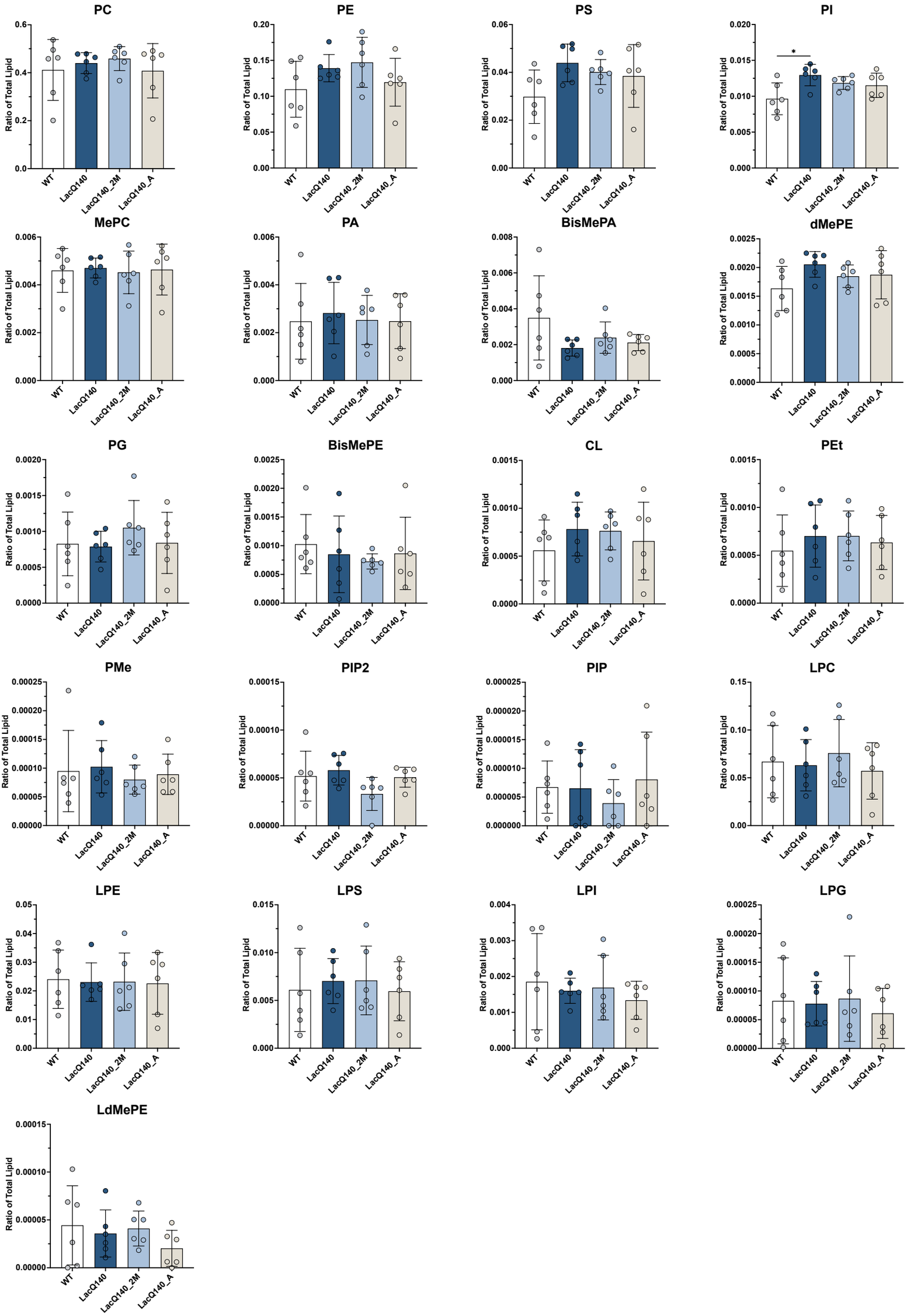

Supplementary Figure 5. Glycerophospholipid subclasses detected in striatum of 6-month-old mice.
Lipids were extracted and analyzed by LC-MS/MS. Graphs show relative intensities for indicated lipid subclasses expressed as a ratio of total lipid intensity per sample for each genotype or treatment group. Plotted values represent summed lipid subclass intensity standardized to total amount of lipid detected in the same sample. Bar charts underneath individual points represent group means and error bars are ± standard deviation. The subclass phosphatidylinositol (PI) was significantly increased in striatum of 6-month-old LacQ140 mice compared to WT mice (One-way ANOVA with Tukey's multiple comparisons test, F (3, 20) = 4.176, * P=0.0189, n=6). This increase is not significant when p-values are adjusted for multiple testing using the Benjamini, Krieger and Yekutieli procedure with a false discovery rate of 5%, (q = 0.7144, n=36). No changes between groups were found in any other glycerophospholipid subclasses. Abbreviations: Phosphatidylcholine (PC), Phosphatidylethanolamine (PE), Phosphatidylserine (PS), Phosphatidylinositol (PI), Methylphosphocholine (MePC), Phosphatidic acid (PA), Bis-methyl phosphatidic acid (BisMePA), Dimethyl phosphatidylethanolamine (dMePE), Phosphatidylgylcerol (PG), Bis-methyl phosphatidyl ethanolamine (BisMePE), Cardiolipin (CL), Phosphatidylethanol (PEt), Phosphatidylmethanol (PMe), Phosphatidylinositol-bisphosphate (PIP2), Phosphatidylinositol-monophosphate (PIP), Lysophosphatidylcholine (LPC), Lysophosphatidylethanolamine (LPE), Lysophosphatidylserine (LPS), Lysophosphatidylinositol (LPI), Lysophosphophosphatidylgylcerol (LPG), Lysodimethyl phosphatidyl ethanolamine (LdMePE).

Supplementary Figure 6

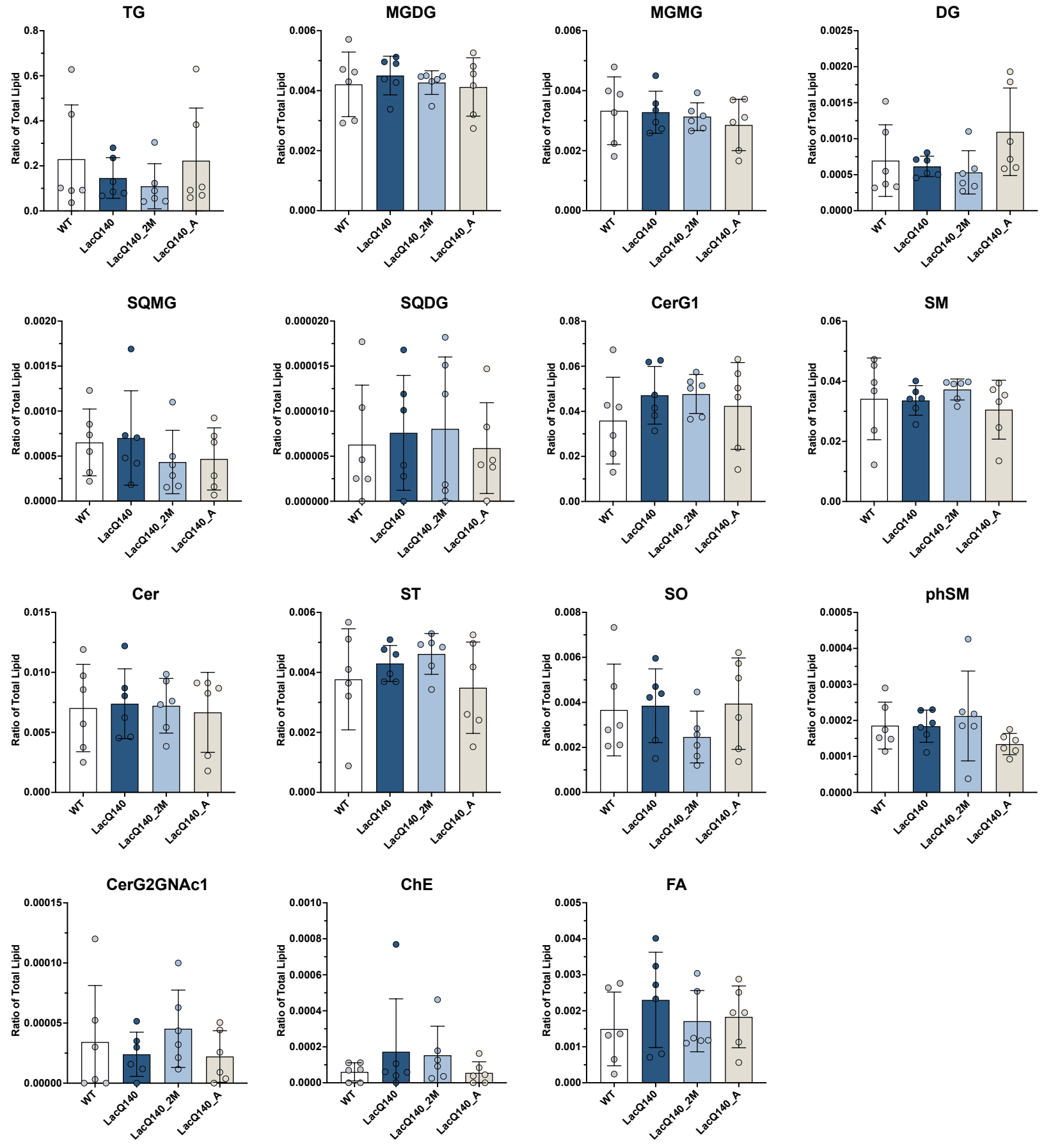

Supplementary Figure 6. Glycerolipid, sphingolipid, sterol lipid, fatty acyl subclasses detected in striatum of 6-month-old mice.

Lipids were extracted and analyzed by LC-MS/MS. Graphs show relative intensities for indicated lipid subclasses expressed as a ratio of total lipid intensity per sample for each genotype or treatment group. Plotted values represent summed lipid subclass intensity standardized to total amount of lipid detected in the same sample. Bar charts underneath individual points represent group means and error bars are ± standard deviation. No changes between groups were found in any glycerolipid, sphingolipid, sterol lipid, or fatty acyl subclasses (One-way ANOVA with Tukey's multiple comparison test, n=6). Abbreviations: *Glycerolipids:* Triglyceride (TG), Monogalactosyldiacylglycerol (MGDG), Monogalactosylmonoacylglycerol (MGMG), Diglyceride (DG), Sulfoquinovosylmonoacylglycerol (SQMG), Sulfoquinovosyldiacylglycerol (SQDG), *Sphingolipids:* Simple Glc series (CerG1), Sphingomyelin (SM), Ceramide (Cer), Sulfatide (ST), Sphingoid base (So), Sphingomyelin phytosphingosine (phSM), Simple Glc series (CerG2GNAc1), *Sterol lipids:* Cholesterol ester (ChE), *Fatty acyls:* Fatty acid (FA).

Supplementary Figure 7

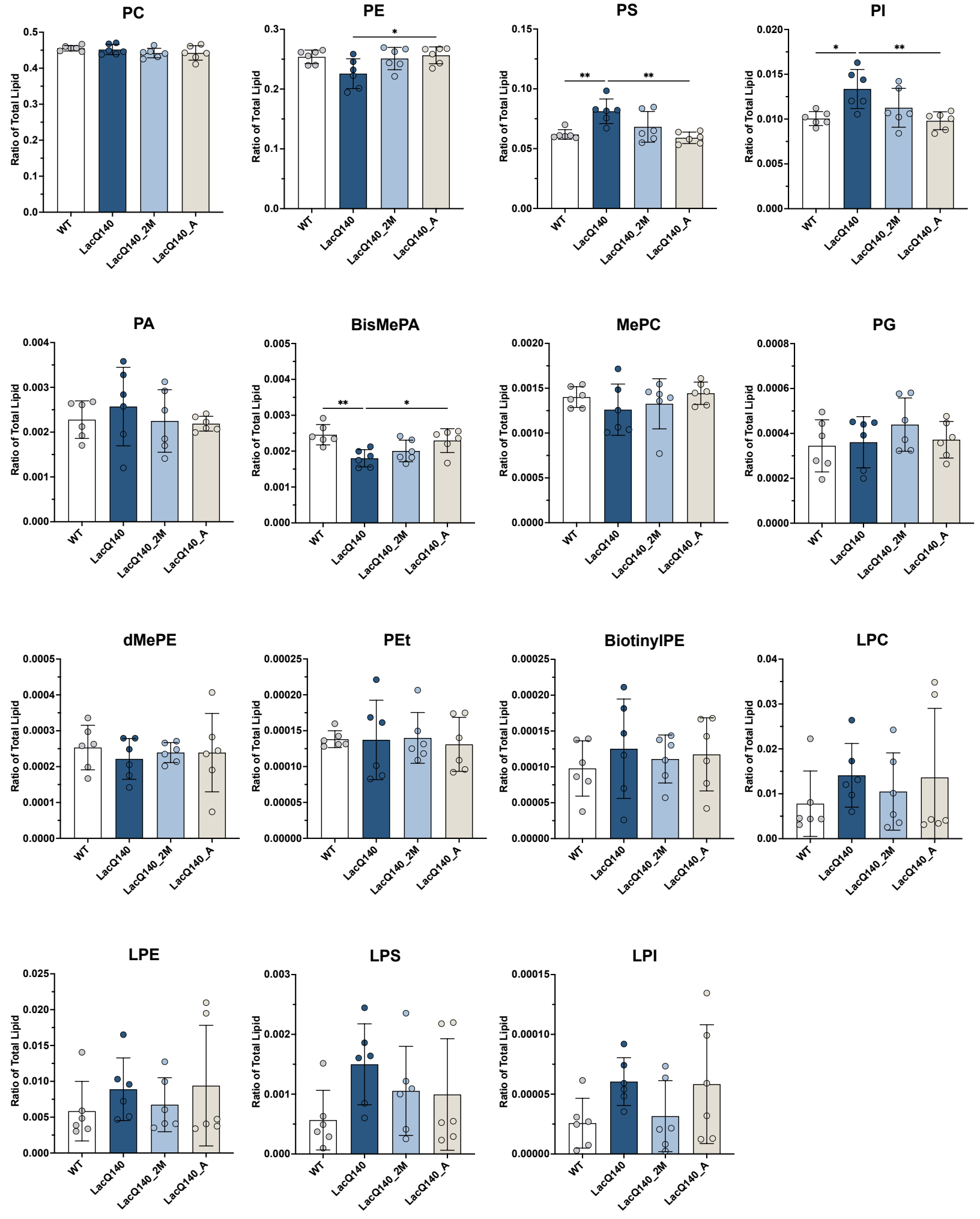

Supplementary Figure 7. Glycerophospholipid subclasses detected in striatum of 9-month-old mice.
Lipids were extracted and analyzed by LC-MS/MS. Graphs show relative intensities for indicated lipid subclasses expressed as a ratio of total lipid intensity per sample for each genotype or treatment group. Plotted values represent summed lipid subclass intensity standardized to total amount of lipid detected in the same sample. Bar charts underneath individual points represent group means and error bars are ± standard deviation. One-way analysis of variance (ANOVA) was used to evaluate differences in lipid subclass intensity between groups and Tukey's multiple comparisons test was used for post-hoc pairwise comparisons (N = 6 mice per group, *p < 0.05, **p < 0.01, Tukey's multiple comparisons test). To correct for multiple testing the Benjamini, Krieger and Yekutieli procedure was used with a false discovery rate of 5% (n=24) and FDR adjusted p-values are reported as q values. The subclass Phosphatidylethanolamine (PE) was not significantly different between LacQ140 and WT mice, however LacQ140_A mice displayed increased PE compared to LacQ140 mice (One-way ANOVA with Tukey's multiple comparison test, F (3, 20) = 3.717, *P=0.0284). This increase was no longer significant after p-values were corrected (q=0.0563). Phosphatidylserine (PS), Phosphatidylinositol (PI), and Bis-methyl phosphatidic acid (BisMePA) are described in **Figure 7**, PS: F (3, 20) = 7.60, **P=0.0014, q=0.0125, **i,** PI: F (3, 20) = 5.707, **P=0.0054, q=0.0168, **j,** BisMePA: F (3, 20) = 6.086, **P=0.0041, q=0.0168. Abbreviations: Phosphatidylcholine (PC), Phosphatidylethanolamine (PE), Phosphatidylserine (PS), Phosphatidylinositol (PI), Phosphatidic acid (PA), Bis-methyl phosphatidic acid (BisMePA), Methylphosphocholine (MePC), Phosphatidylgylcerol (PG), Dimethyl phosphatidylethanolamine (dMePE), Phosphatidylethanol (PEt), Biotinyl-phosphoethanolamine (BiotinylPE), Lysophosphatidylcholine (LPC), Lysophosphatidylethanolamine (LPE), Lysophosphatidylserine (LPS), Lysophosphatidylinositol (LPI).

Supplementary Figure 8

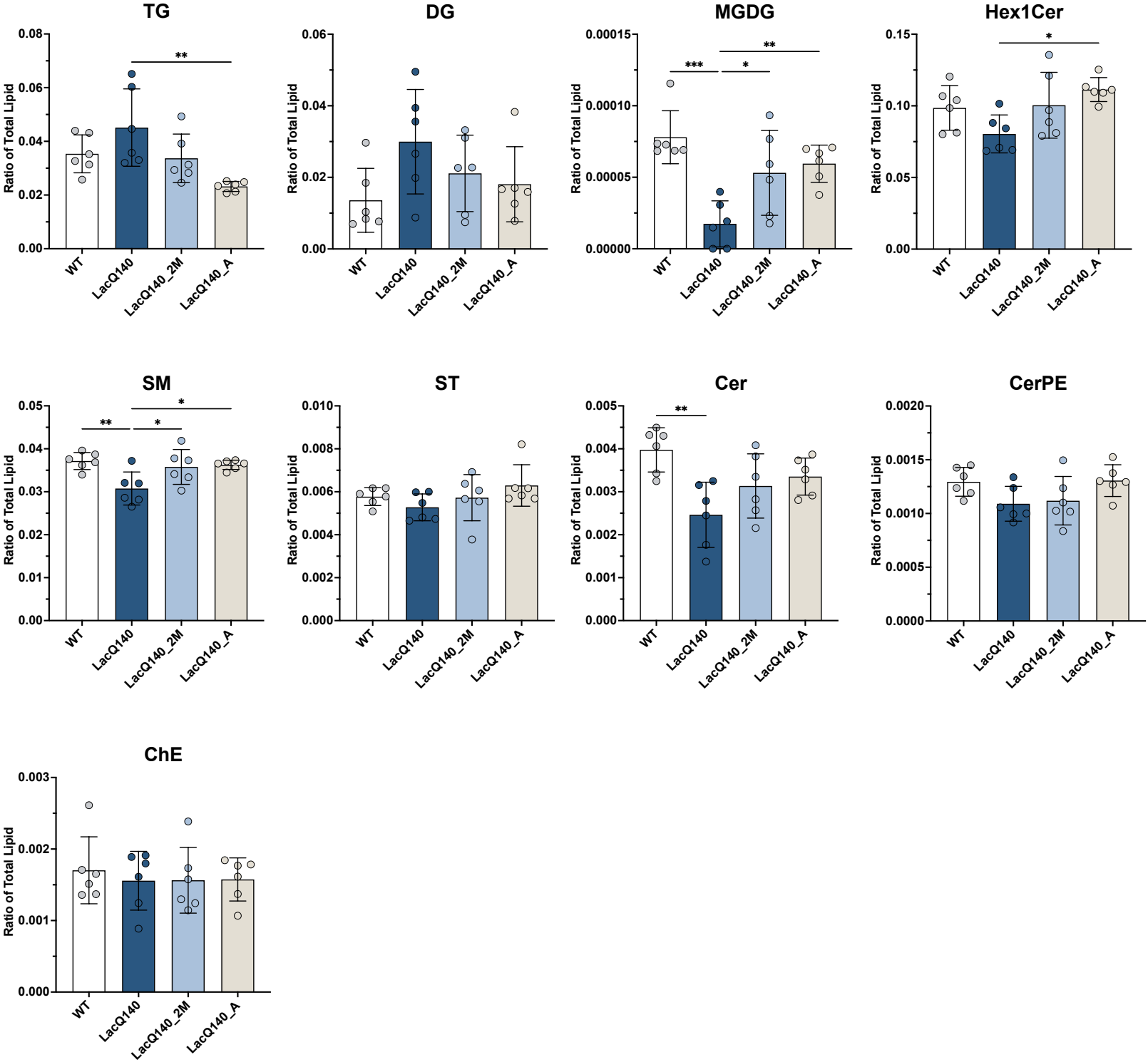

Supplementary Figure 8. Glycerolipid, sphingolipid, and sterol lipid subclasses detected in striatum of 9-month-old mice.

Lipids were extracted and analyzed by LC-MS/MS. Graphs show relative intensities for indicated lipid subclasses expressed as a ratio of total lipid intensity per sample for each genotype or treatment group. Plotted values represent summed lipid subclass intensity standardized to total amount of lipid detected in the same sample. Bar charts underneath individual points represent group means and error bars are ± standard deviation. One-way analysis of variance (ANOVA) was used to evaluate differences in lipid subclass intensity between groups and Tukey's multiple comparisons test was used for post-hoc pairwise comparisons (N = 6 mice per group, *p < 0.05, **p < 0.01, ***p < 0.001, Tukey's multiple comparisons test). To correct for multiple testing the Benjamini, Krieger and Yekutieli procedure was used with a false discovery rate of 5% (n=24), FDR adjusted p-values are reported as q values. The glycerolipid subclass triglyceride (TG) was unchanged between LacQ140 and WT mice, however, LacQ140_A mice displayed decreased levels of TG compared to LacQ140 mice. (One-way ANOVA with Tukey's multiple comparison test F (3, 20) = 5.637, **P=0.0057, q=0.0168). The sphingolipid subclass Hexosylceramide (Hex1Cer) was unchanged between LacQ140 and WT mice but LacQ140_A mice displayed increased levels of Hex1Cer compared to LacQ140 mice (One-way ANOVA with Tukey's multiple comparison test (3, 20) = 3.891, *P=0.0243). This increase in Hex1Cer no longer significant after p-values were corrected (q=0.0542). Monogalactosyldiacylglycerol (MGDG), Sphingomyelin (SM) and Ceramide (Cer) are described in **Figure 7**, MGDG: F (3, 20) = 9.350, ***P=0.0005, q=0.0089, SM: F (3, 20) = 5.465, **P=0.0066, q=0.0168, Cer: F (3, 20) = 5.883, **P=0.00480, q=0.0168. Abbreviations: *Glycerolipids:* Triglyceride (TG), Diglyceride (DG), Monogalactosyldiacylglycerol (MGDG), *Sphingolipids:* Hexosylceramide (Hex1Cer), Sphingomyelin (SM), Sulfatide (ST), Ceramide (Cer), Ceramide phosphorylethanolamine (CerPE), Sterol lipids: Cholesterol ester (ChE).

Supplementary Figure 9

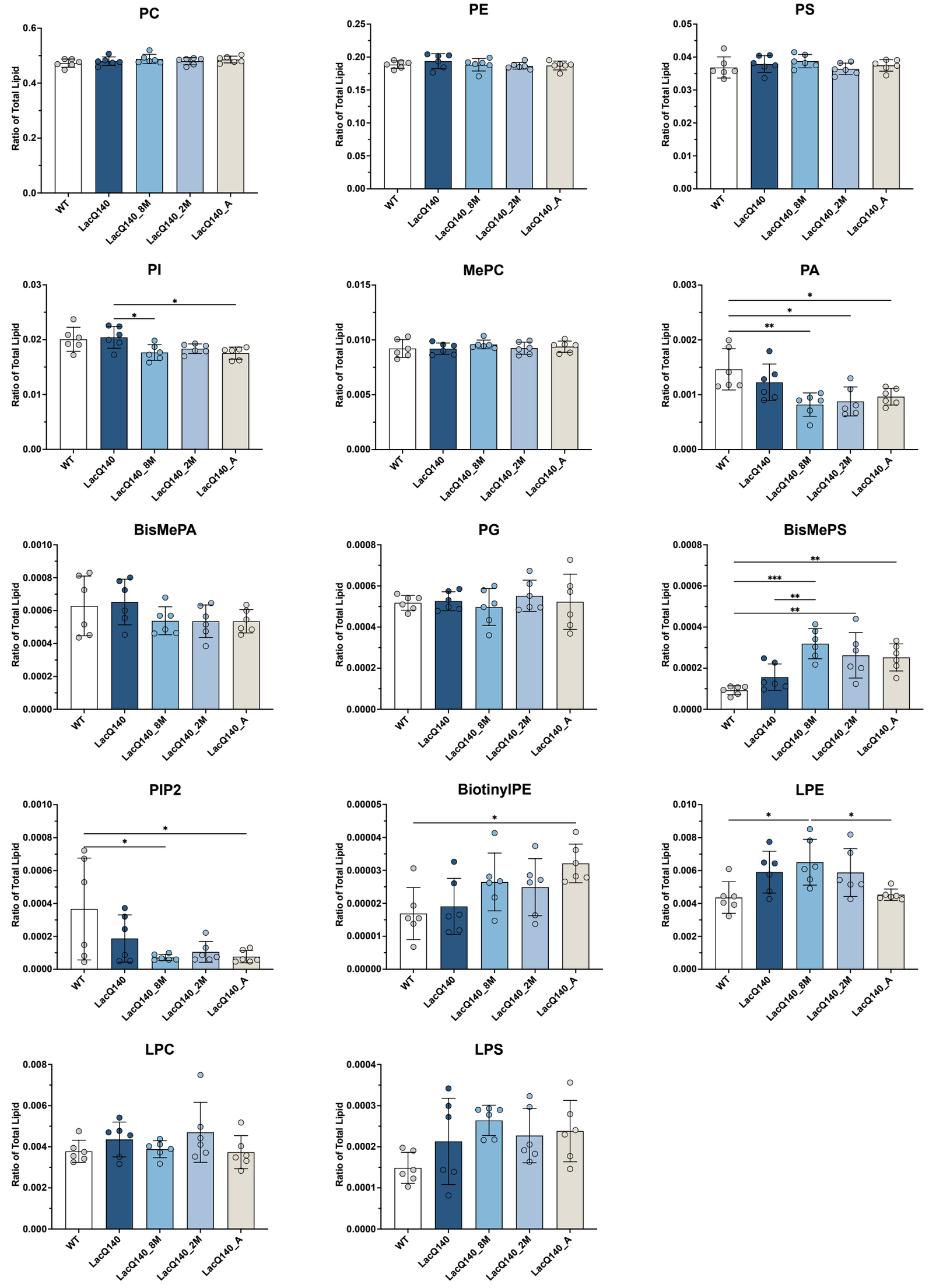

Supplementary Figure 9. Glycerophospholipid subclasses detected in striatum of 12-month-old mice.
Lipids were extracted and analyzed by LC-MS/MS. Graphs show relative intensities for indicated lipid subclasses expressed as a ratio of total lipid intensity per sample for each genotype or treatment group. Plotted values represent summed lipid subclass intensity standardized to total amount of lipid detected in the same sample. Bar charts underneath individual points represent group means and error bars are ± standard deviation. One-way analysis of variance (ANOVA) was used to evaluate differences in lipid subclass intensity between groups and Tukey's multiple comparisons test was used for post-hoc pairwise comparisons (N = 6 mice per group, *p < 0.05, **p < 0.01, ***p < 0.001, Tukey's multiple comparisons test). To correct for multiple testing the Benjamini, Krieger and Yekutieli procedure was used with a false discovery rate of 5% (n=29), FDR adjusted p-values are reported as q values. Phosphatidylinositol (PI) was decreased in both LacQ140_8M and LacQ140_A mice compared to LacQ140 mice (F (4, 25) = 4.316, **P=0.0086, q=0.0338). Phosphatidic acid (PA) was decreased in LacQ140_8M, LacQ140_2M, and LacQ140_A mice compared to WT mice (F (4, 25) = 5.537, **P=0.0025, q=0.0184). Bis-methylphosphatidylserine (BisMePS) was increased in LacQ140_8M, LacQ140_2M, and LacQ140_A mice compared to WT mice. Additionally, it was increased in LacQ140_2M mice compared to LacQ140 mice (F (4, 25) = 9.308, ****P<0.0001, q=0.0022). Phosphatidylinositol-bisphosphate (PIP2) was decreased in LacQ140_8M and LacQ140_A mice compared to WT mice (F (4, 25) = 3.743, *P=0.0161, q=0.0394). Biotinyl-phosphoethanolamine (BiotinylPE) was increased in LacQ140_A mice compared to WT mice (F (4, 25) = 3.446, *P=0.0225, q=0.0451). Lysophosphatidylethanolamine (LPE) was increased in LacQ140_8M mice compared to WT mice and decreased in LacQ140_A mice compared to LacQ140_8M mice (F (4, 25) = 3.957, *P=0.0127, q=0.035). Abbreviations: Phosphatidylcholine (PC), Phosphatidylethanolamine (PE), Phosphatidylserine (PS), Phosphatidylinositol (PI), Methylphosphocholine (MePC), Phosphatidic acid (PA), Bis-methyl phosphatidic acid (BisMePA), Phosphatidylgylcerol (PG), Bis-methylphosphatidylserine (BisMePS), Phosphatidylinositol-bisphosphate (PIP2), Biotinyl-phosphoethanolamine (BiotinylPE), Lysophosphatidylethanolamine (LPE), Lysophosphatidylcholine (LPC), Lysophosphatidylserine (LPS).

Supplementary Figure 10

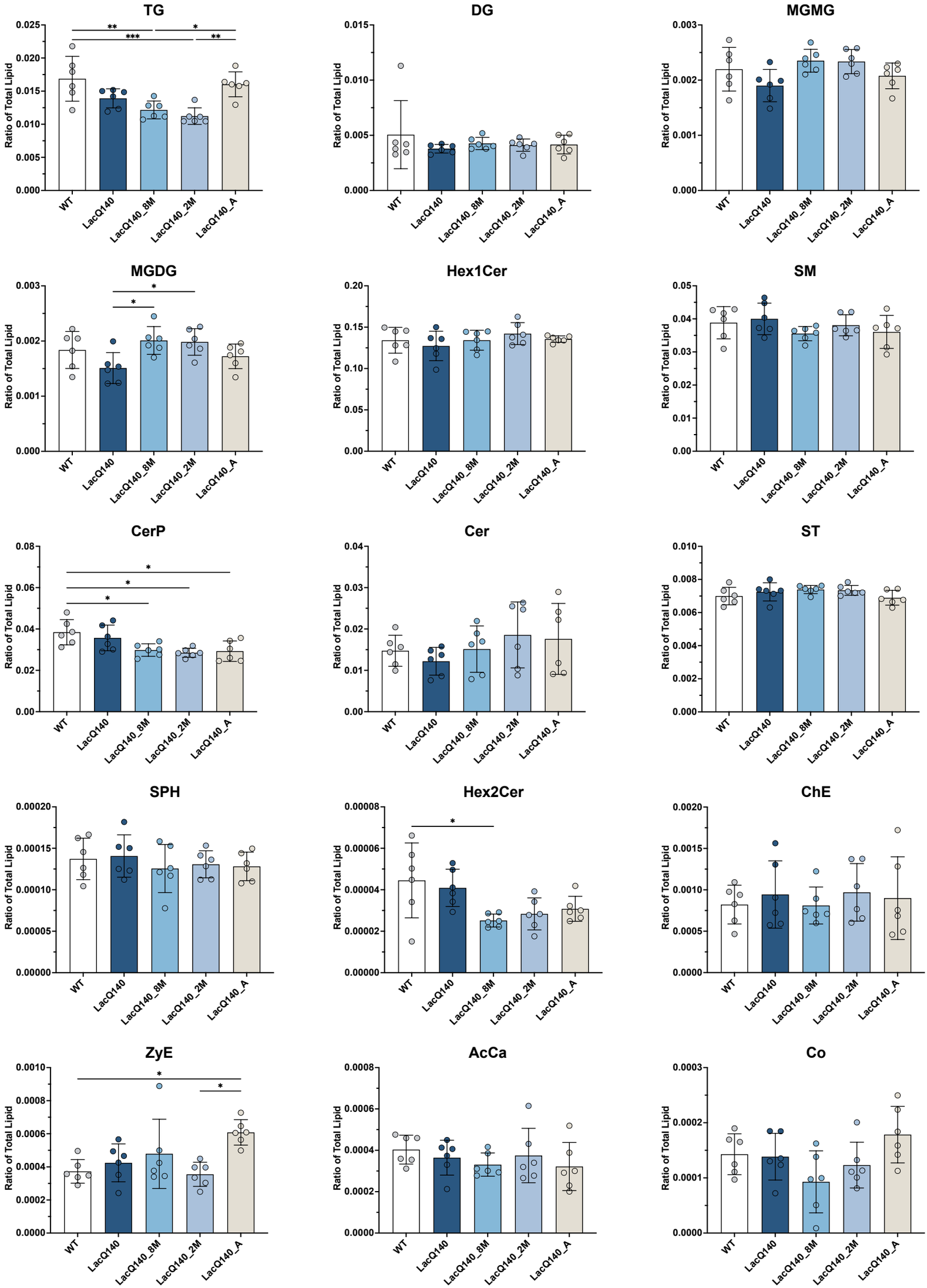

Supplementary Figure 10. Glycerolipid, sphingolipid, sterol lipid, fatty acyl, and prenol lipid subclasses detected in striatum of 12-month-old mice.

Lipids were extracted and analyzed by LC-MS/MS. Graphs show relative intensities for indicated lipid subclasses expressed as a ratio of total lipid intensity per sample for each genotype or treatment group. Plotted values represent summed lipid subclass intensity standardized to total amount of lipid detected in the same sample. Bar charts underneath individual points represent group means and error bars are ± standard deviation. One-way analysis of variance (ANOVA) was used to evaluate differences in lipid subclass intensity between groups and Tukey's multiple comparisons test was used for post-hoc pairwise comparisons (N = 6 mice per group, *p < 0.05, **p < 0.01, ***p < 0.001, Tukey's multiple comparisons test). To correct for multiple testing the Benjamini, Krieger and Yekutieli procedure was used with a false discovery rate of 5% (n=29), FDR adjusted p-values are reported as q values.The glycerolipid subclass Triglyceride (TG) was decreased in LacQ140_8M and LacQ140_2M mice compared to WT mice. In addition, LacQ140_A mice had increased levels of TG compared to LacQ140_8M and LacQ140_2M mice (F (4, 25) = 8.593, ***P=0.0002, q=0.0022). Monogalactosylmonoacylglycerol (MGMG) was significantly different by One-way ANOVA (no longer significant following correction) and Tukey's multiple comparisons test did not reveal any significant differences between groups (F (4, 25) = 2.765, *P=0.0497, q=0.0887, ns). Monogalactosyldiacylglycerol (MGDG) was increased in LacQ140_8M and LacQ140_2M mice compared to LacQ140 mice (F (4, 25) = 3.491, *P=0.0214, q=0.0451). The sphingolipid subclass Ceramide phosphate (CerP) was decreased in LacQ140_8M and LacQ140_2M, and LacQ140_A mice compared to WT mice (F (4, 25) = 5.185, **P=0.0035, q=0.0193). Dihexosylceramide (Hex2Cer) was decreased in LacQ140_8M mice compared to WT mice (F (4, 25) = 4.076, *P=0.0112, q=0.035). The sterol lipid subclass Zymosterol (ZyE) was increased in LacQ140_A mice compared to WT mice and compared to LacQ140_2M mice (F (4, 25) = 4.256, **P=0.0092, q= 0.0338).Abbreviations: *Glycerolipids:* Triglyceride (TG), Diglyceride (DG), Monogalactosylmonoacylglycerol (MGMG), Monogalactosyldiacylglycerol (MGDG), *Sphingolipids:* Hexosylceramide (Hex1Cer), Sphingomyelin (SM), Ceramide phosphate (CerP), Ceramide (Cer), Sulfatide (ST), Sphingosine (SPH), Dihexosylceramide (Hex2Cer), Sterol lipids: Cholesterol ester (ChE), Zymosterol (ZyE), *Fatty acyls:* Acyl Carnitine (AcCa), *Prenol lipids:* Coenzyme (Co).

Supplementary Figure 11

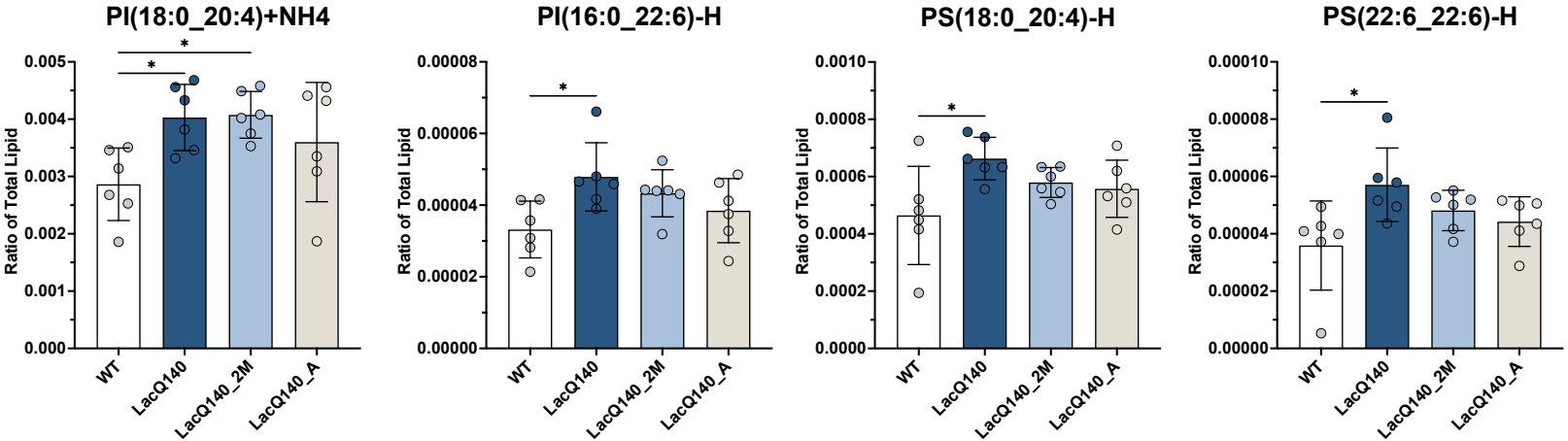

Supplementary Figure 11. Individual lipid species significantly different between 6-month-old LacQ140 and WT mice (p<0.05).

Lipids were extracted and analyzed by LC-MS/MS. Graphs show relative intensities for indicated lipid species expressed as a ratio of total lipid intensity per sample for each genotype or treatment group. Plotted values represent individual lipid species intensity standardized to total amount of lipid detected in the same sample. Bar charts underneath individual points represent group means and error bars are ± standard deviation. One-way analysis of variance (ANOVA) was used to evaluate differences in lipid species intensity between groups and Tukey's multiple comparisons test was used for post-hoc pairwise comparisons (N = 6 mice per group, *p < 0.05, Tukey's multiple comparisons test). To correct for multiple testing over all lipids analyzed, the Benjamini, Krieger and Yekutieli procedure was used with a false discovery rate of 5% (n=800), FDR adjusted p-values are reported as q values. No individual species found to be different by one-way ANOVA were significant following correction of p-values. Additional statistical details are available in **Supplemental Table 1** and **Prism File A.** Abbreviations: *Glycerophospholipids:* Phosphatidylinositol (PI), Phosphatidylserine (PS)

Supplementary Figure 12

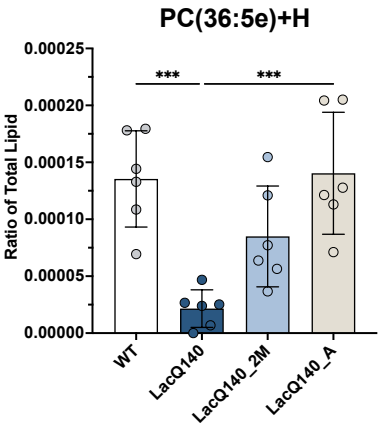

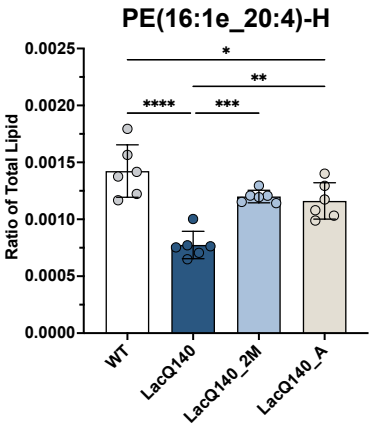

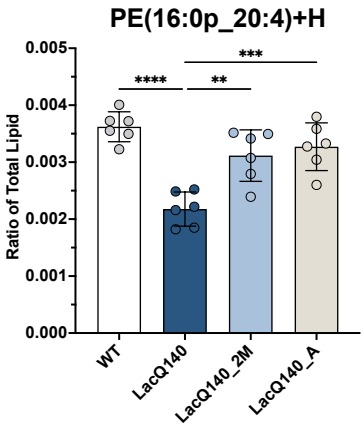

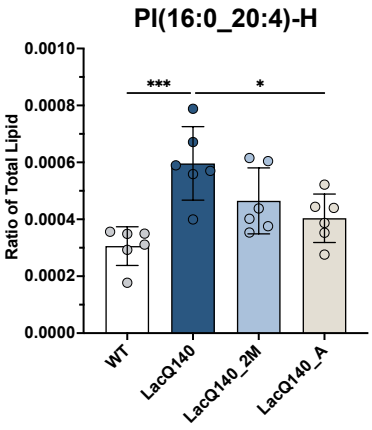

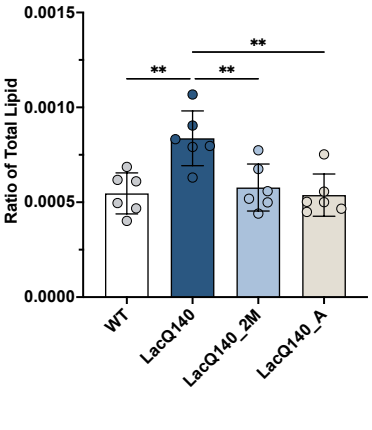

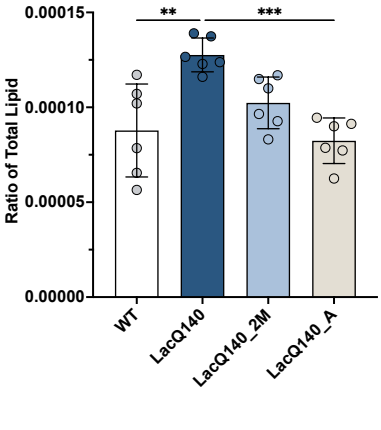

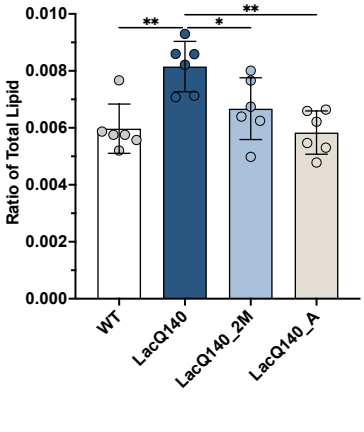

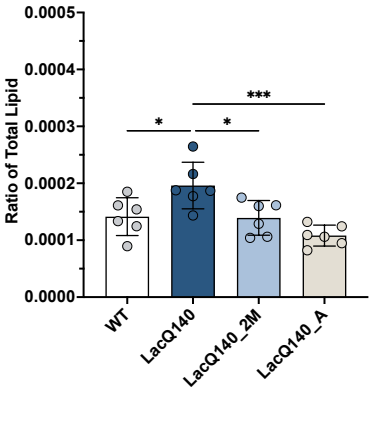

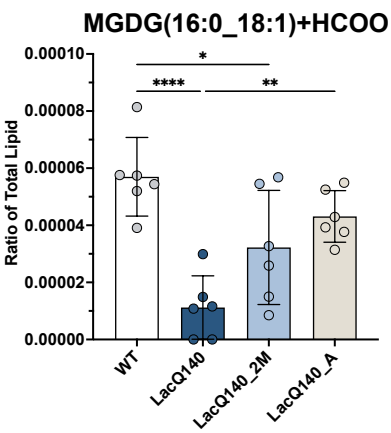

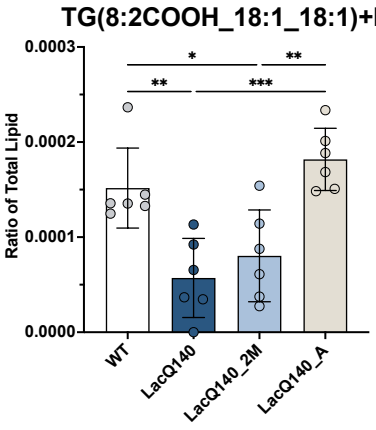

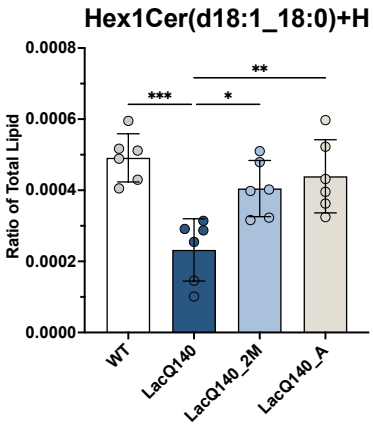

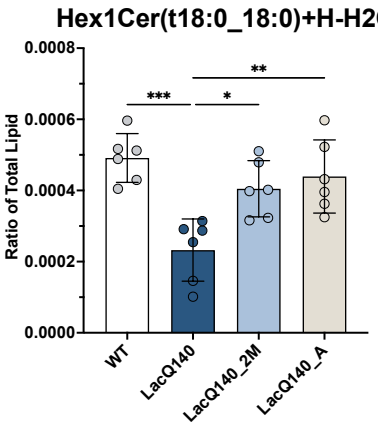

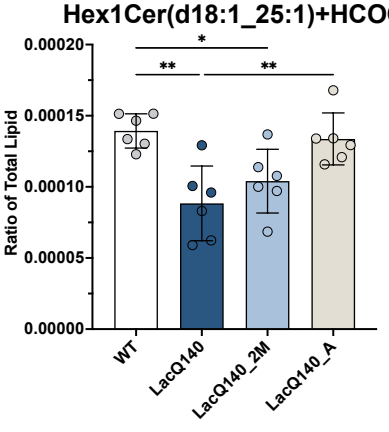

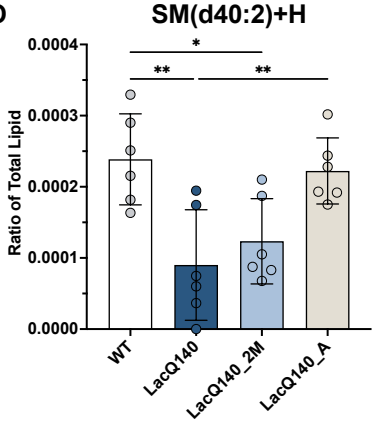

Supplementary Figure 12. Individual lipid species significantly different between 9-month-old LacQ140 and WT mice (q<0.05).

Lipids were extracted and analyzed by LC-MS/MS. Graphs show relative intensities for indicated lipid species expressed as a ratio of total lipid intensity per sample for each genotype or treatment group. Plotted values represent individual lipid species intensity standardized to total amount of lipid detected in the same sample. Bar charts underneath individual points represent group means and error bars are ± standard deviation. One-way analysis of variance (ANOVA) was used to evaluate differences in lipid species intensity between groups and Tukey's multiple comparisons test was used for post-hoc pairwise comparisons (N = 6 mice per group, *p < 0.05, **p < 0.01, ***p < 0.001, ****p < 0.0001, Tukey's multiple comparisons test). To correct for multiple testing over all lipids analyzed, the Benjamini, Krieger and Yekutieli procedure was used with a false discovery rate of 5% (n=632), FDR adjusted p-values are reported as q values. Additional statistical details are available in **Supplementary Table 2** and **Prism File B.** Abbreviations: *Glycerophospholipids:* Phosphatidylcholine (PC), Phosphatidylethanolamine (PE), Phosphatidylinositol (PI), Phosphatidylserine (PS), *Glycerolipids:* Monogalactosyldiacylglycerol (MGDG), Triglyceride (TG), *Sphingolipids:* Hexosylceramide (Hex1Cer), Sphingomyelin (SM).

Supplementary Figure 13

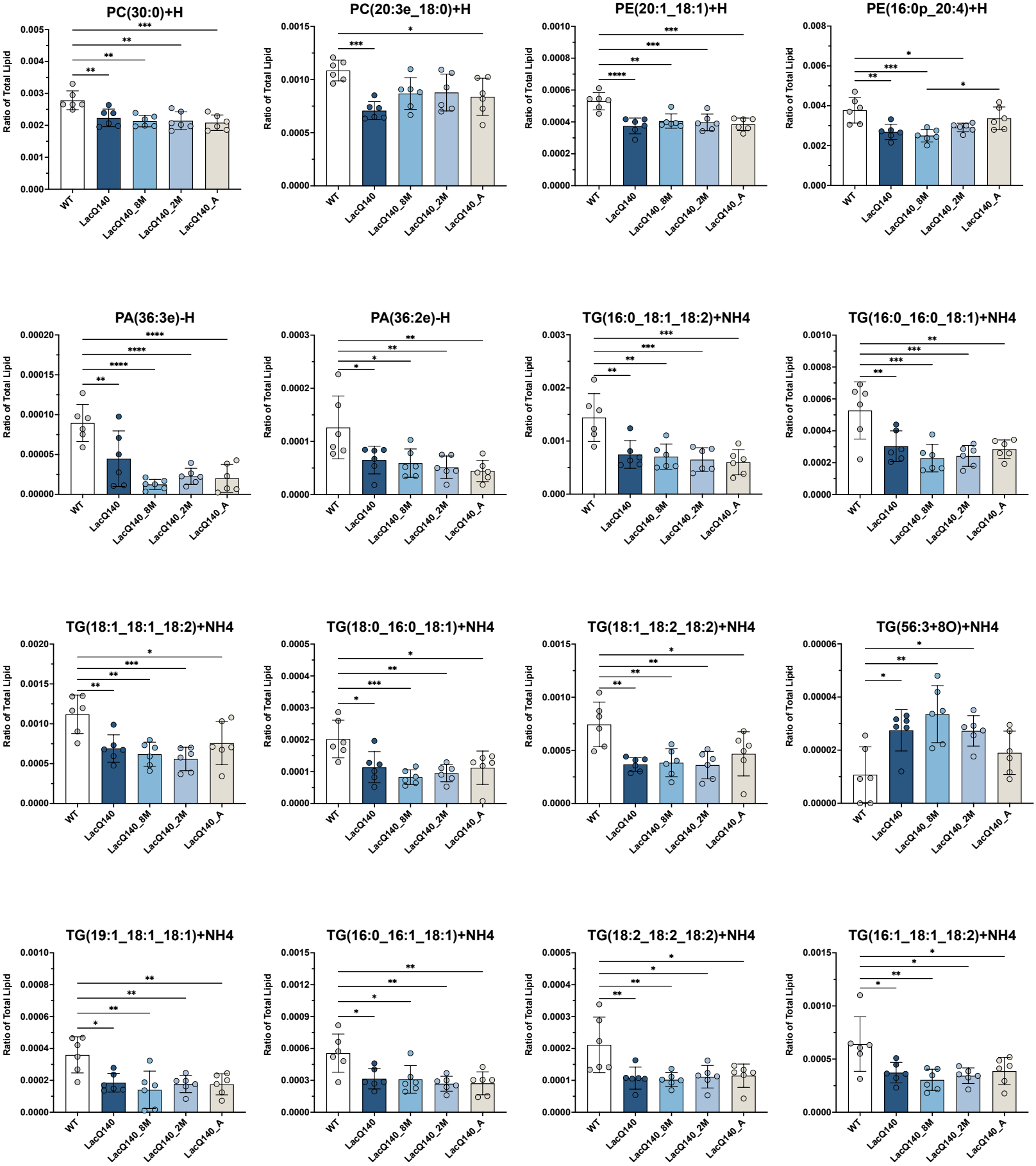

Supplementary Figure 13. Glycerophospholipid and glycerolipid individual lipid species significantly different between 12-month-old LacQ140 and WT mice (q<0.05).

Lipids were extracted and analyzed by LC-MS/MS. Graphs show relative intensities for indicated lipid species expressed as a ratio of total lipid intensity per sample for each genotype or treatment group. Plotted values represent individual lipid species intensity standardized to total amount of lipid detected in the same sample. Bar charts underneath individual points represent group means and error bars are ± standard deviation. One-way analysis of variance (ANOVA) was used to evaluate differences in lipid species intensity between groups and Tukey's multiple comparisons test was used for post-hoc pairwise comparisons (N = 6 mice per group, *p < 0.05, **p < 0.01, ***p < 0.001, ****p < 0.0001, Tukey's multiple comparisons test). To correct for multiple testing over all lipids analyzed, the Benjamini, Krieger and Yekutieli procedure was used with a false discovery rate of 5% (n=735), FDR adjusted p-values are reported as q values. Additional statistical details are available in **Supplementary Table 3** and **Prism File C**.

Abbreviations: *Glycerophospholipids:* Phosphatidylcholine (PC), Phosphatidylethanolamine (PE), Phosphatidic acid (PA), *Glycerolipids:* Triglyceride (TG).

Supplementary Figure 14

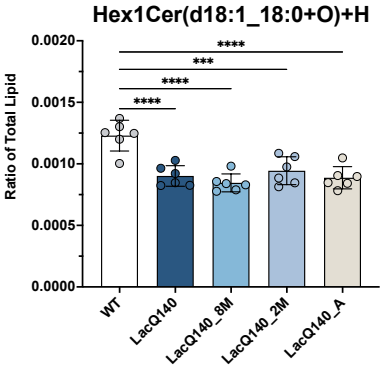

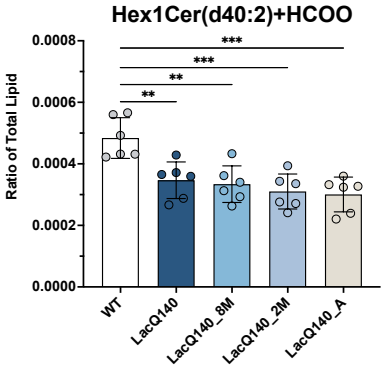

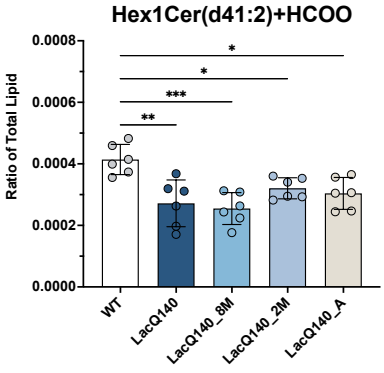

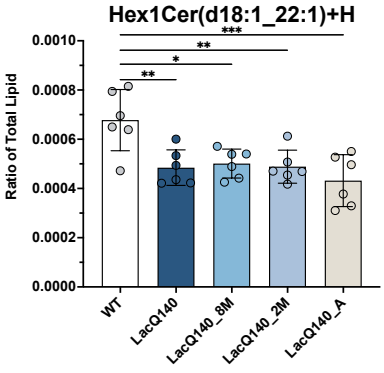

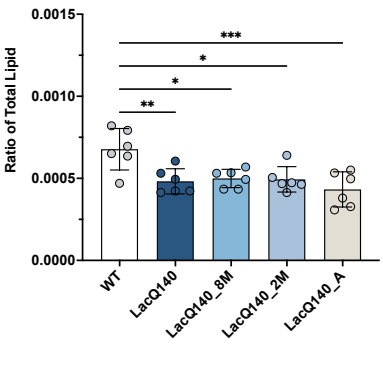

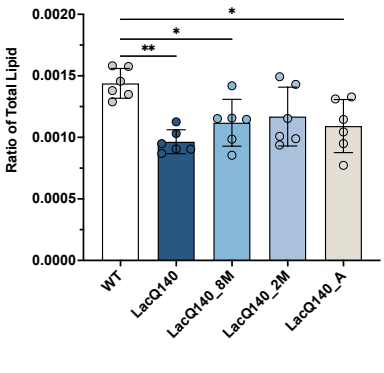

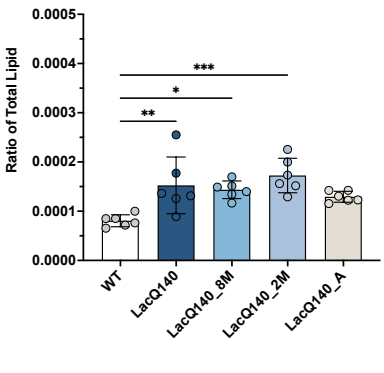

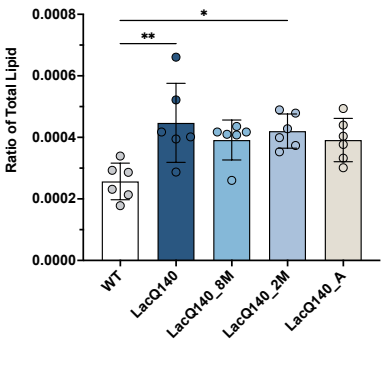

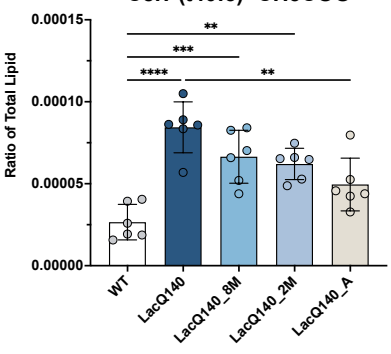

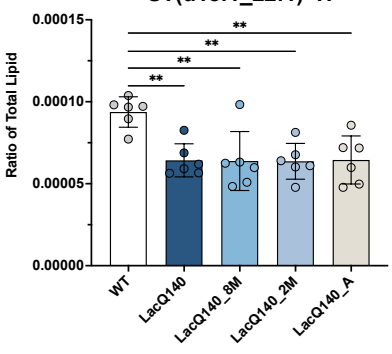

Supplementary Figure 14. Sphingolipid individual lipid species significantly different between 12-month-old LacQ140 and WT mice (q<0.05).

Lipids were extracted and analyzed by LC-MS/MS. Graphs show relative intensities for indicated lipid species expressed as a ratio of total lipid intensity per sample for each genotype or treatment group. Plotted values represent individual lipid species intensity standardized to total amount of lipid detected in the same sample. Bar charts underneath individual points represent group means and error bars are ± standard deviation. One-way analysis of variance (ANOVA) was used to evaluate differences in lipid species intensity between groups and Tukey's multiple comparisons test was used for post-hoc pairwise comparisons (N = 6 mice per group, *p < 0.05, **p < 0.01, ***p < 0.001, ****p < 0.0001 Tukey's multiple comparisons test). To correct for multiple testing over all lipids analyzed, the Benjamini, Krieger and Yekutieli procedure was used with a false discovery rate of 5% (n=735), FDR adjusted p-values are reported as q values. Additional statistical details are available in **Supplementary Table 3** and **Prism File C.** Abbreviations: *Sphingolipids:* Hexosylceramide (Hex1Cer), Sphingomyelin (SM), Ceramide phosphate (CerP), Sulfatide (ST).

Supplemetary Figure 15

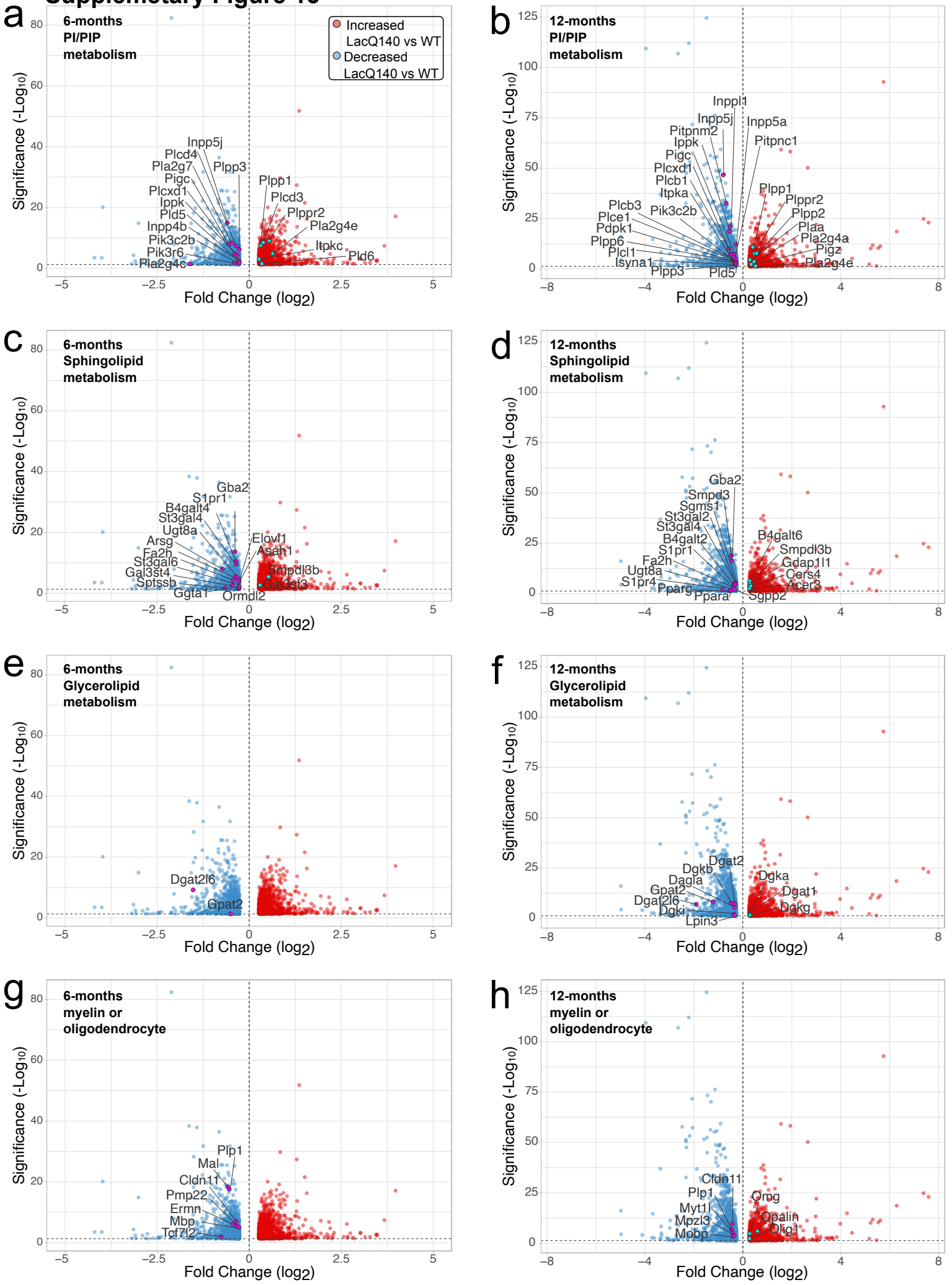

Supplementary Figure 15. Differentially expressed striatal transcripts related to sphingolipid metabolism, PI/PIP metabolism, glycerolipid metabolism, and myelin or oligodendrocytes in 6-and 12-month-old LacQ140 mice.
RNA sequencing data in the LacQ140 model (GEO GSE156236) was manually curated to identify differentially expressed transcripts related to **(a,b)** phosphatidylinositol (PI)/ phosphatidylinositol-phosphate (PIP) metabolism, **(c,d)** sphingolipid metabolism, **(e,f)** glycerolipid metabolism, and **(g,h)** myelin or oligodendrocytes. At the 6-month timepoint, 2711 differentially expressed genes (DEG) were detected between LacQ140 (n=5 males, n=5 females) and WT (n=5 males, n=5 females) groups. At the 12-month timepoint, 2989 DEGs were detected between LacQ140 (n=5 males, n=5 females) and WT (n=5 males, n=5 females) groups. Volcano plots were generated from the DEG list (fold change greater than 20% in either direction with an FDR adjusted p-value<0.05 were considered differentially expressed) using VolcaNoseR software (Goedhart & Luijsterburg, 2020). Red dots indicate genes that were upregulated in LacQ140 compared to WT, whereas blue dots indicate genes that were downregulated in LacQ140 compared to WT. Pink dots with annotations show downregulated genes and cyan dots show upregulated genes related to the indicated biological process. FDR adjusted p-values from the DEG list are -log10 transformed and fold changes are log2 transformed.